Roosa Kalliovalkama

# Decarbonizing Microgrids: Techno-Economic Analysis of Hybrid Hydrogen Systems

School of Technology and Innovations
Master’s thesis in Smart Energy Program

Turku 2024

**UNIVERSITY OF VAASA**
**School of Technology and Innovations**
**Author:** Roosa Kalliovalkama
**Title of the Thesis:** Decarbonizing Microgrids: Techno-Economic Analysis of Hybrid Hydrogen Systems
**Degree:** Master of Science in Technology
**Discipline:** Smart Energy
**Supervisor:** Professor Xiaoshu Lü
**Year:** 2024 **Pages:** 111

**ABSTRACT:**

Decarbonizing the energy sector is recognized as essential by the European Union for reducing global greenhouse gas emissions, with green hydrogen positioned as a cornerstone of the carbon neutrality goals. Hybrid hydrogen systems, which integrate solar, wind, and storage technologies, are increasingly identified for their potential in microgrid applications, providing a viable pathway toward sustainable energy solutions.

A detailed techno-economic analysis is conducted in this thesis to evaluate the technical feasibility and economic performance of green hybrid hydrogen systems considering influential factors like regions, climates, and infrastructure. Key performance indicators (KPIs), including the Levelized Cost of Energy (LCOE), Levelized Cost of Hydrogen (LCOH), and the proportion of excess electricity generated, are employed to assess the efficiency and viability of the systems under diverse operational conditions. Emphasis is placed on factors such as resource availability and operating hours, which are found to significantly influence the design and performance of microgrid systems.

Nine microgrid configurations are modelled and simulated using the HOMER Pro optimization software. Technical specifications, economic assumptions, and environmental conditions are defined and reviewed as part of the system modelling process. The *Trial-and-Test Method* approach is applied to determine the component capacities.

Results show that the KPIs are influenced by a range of factors, such as the wind and solar resources and microgrid component capacities. Noteworthy variations in the KPIs are found between the region's different climates. Once the utilization of solar sources was favored in RESs relation, both the LCOE and LCOH cost values increased substantially, due to the increase in Capital Expenditure (CAPEX) and Fixed Operation and Maintenance (FOM) costs.

The analysis underscored the role of location and operational profiles in influencing microgrid performance and cost outcomes, which varied across the case studies. The LCOE and LCOH values exhibited considerable variation, with some values being up to twice as high as the lowest ones. Limitations and potential directions for future research are also suggested in this thesis, as the observed KPI values exceeded those reported in the literature. A comprehensive understanding of key factors, including geographic location, resource availability, and operational hours, along with their effective implementation, is essential for optimizing green hybrid hydrogen systems, ensuring the efficient operation of microgrid configurations, and advancing the global adoption of renewable energy technologies.

**KEYWORDS:** Decarbonization, Renewable Energy, Hydrogen, Case Studies, Techno-Economic Analysis, Trial-and-Test Method, HOMER Pro, Electricity Generation.

**VAASAN YLIOPISTO**
**Tekniikan ja innovaatiojohtamisen yksikkö**
**Tekijä:** Roosa Kalliovalkama
**Tutkielman nimi:** Decarbonizing Microgrids: Techno-Economic Analysis of Hybrid Hydrogen Systems
**Tutkinto:** Diplomi-insinööri
**Oppiaine:** Smart Energy
**Työn ohjaaja:** Professori Xiaoshu Lü
**Valmistumisvuosi:** 2024 **Sivumäärä:** 111

**TIIVISTELMÄ:**
Energiajärjestelmien hiilidioksidipäästöjen vähentäminen on Euroopan unionin tunnistama keskeinen tavoite maailmanlaajuisten kasvihuonekaasupäästöjen vähentämiseksi, ja vihreä vety nähdään hiilineutraaliustavoitteiden kulmakivenä. Hybridivetyjärjestelmät, jotka yhdistävät aurinko-, tuuli- ja varastointiteknologioita, ovat yhä useammin tunnistettu lupaaviksi ratkaisuiksi mikroverkkojen sovelluksissa, tarjoten toteuttamiskelpoisen polun kohti kestäviä energiantuotantoratkaisuja.

Tässä opinnäytetyössä suoritetaan teknistaloudellinen analyysi vihreiden hybridivetyjärjestelmien teknisen toteutettavuuden ja taloudellisen suorituskyvyn arvioimiseksi huomioiden alueellisia, ilmastollisia ja infrastruktuurisia tekijöitä. Järjestelmien tehokkuuden ja toteuttamiskelpoisuuden arvioinnissa käytetään keskeisiä suoritusindikaattoreita (KPI), kuten energiantuotannon tasakustannusta (LCOE), vedyn tuotannon tasakustannusta (LCOH) sekä tuotetun ylijäämäsähkön osuutta. Erityistä huomiota kiinnitetään resursseihin ja käyttöaikoihin, joiden todetaan vaikuttavan olennaisesti mikroverkkosovellusten suunnitteluun ja suorituskykyyn.

Yhdeksän mikroverkkokonfiguraatiota mallinnetaan ja simuloidaan HOMER Pro -optimointiohjelmiston avulla. Teknisiä määrityksiä, taloudellisia oletuksia ja ympäristöolosuhteita määritetään ja arvioidaan osana järjestelmän mallinnusprosessia. Komponenttikapasiteettien määrittämisessä sovelletaan *Koetus- ja Testausmenetelmää*.

Tulokset osoittavat, että keskeiset suoritusindikaattorit (KPI) ovat riippuvaisia monista tekijöistä, kuten tuuli- ja aurinkoresursseista sekä mikroverkon komponenttien kapasiteeteista. Huomattavia eroja suoritusindikaattoreissa havaittiin eri alueiden ilmasto-olosuhteiden välillä. Kun uusiutuvien energialähteiden (RES) osalta painotettiin aurinkoresurssien hyödyntämistä, sekä LCOE- että LCOH-kustannusarvot nousivat olennaisesti pääomakustannusten (CAPEX) ja kiinteiden käyttökustannusten (FOM) kasvun seurauksena.

Analyysi korostaa sijainnin ja ajoprofiilien merkitystä mikroverkkojen suorituskyvyn ja kustannusten muotoutumisessa, mikä vaihteli selvästi tapaustutkimusten välillä. LCOE- ja LCOH-arvot osoittivat olennaista vaihtelua, joissakin tapauksissa korkeimmat arvot olivat jopa kaksinkertaisia alhaisimpiin arvoihin verrattuna. Rajoituksia ja mahdollisia tulevaisuuden tutkimussuuntia ehdotetaan myös tässä opinnäytetyössä, sillä havaitut KPI-arvot ylittivät kirjallisuudessa raportoituja arvoja. Keskeisten tekijöiden, kuten maantieteellisen sijainnin, resurssien saatavuuden ja käyttöaikojen, kattava ymmärtäminen sekä niiden tehokas hyödyntäminen ovat olennaisia vihreiden hybridivetyjärjestelmien optimoinnissa, mikroverkkojen tehokkaassa toiminnassa ja kestävien energiateknologien maailmanlaajuisen käyttöönoton edistämisessä.

**AVAINSANAT:** Hiilineutraalius, Uusiutuva Energia, Vety, Tapaustutkimuksia, Teknistaloudellinen Analyysi, Testaus- ja Koetusmenetelmä, HOMER Pro, Sähköntuotanto.

# Preface

Writing a master's thesis is challenging, but certainly not impossible, though at times, it felt as if it might be. The process took a bit longer than I expected, but now that it is complete, I feel excited, happy, and even a little nervous. I am ready to begin a new chapter in my life and, hopefully, to work in the field I am so passionate about.

I have had the absolute pleasure of working on my thesis with the support of an incredible team from Wärtsilä Finland Oy. I am deeply grateful to Rasmus Teir, Johan Ågren, Emil Rönnqvist, and Tuomas Paloviita for the effort, time, and passion you brought to this research project. Thank you, Rasmus, for sharing your specialized knowledge with me; Tuomas, for assisting with the software and technical aspects of this research; and Johan and Emil, for your encouragement and support throughout the entire thesis process. Without your help, this journey would have been nearly impossible. You shared your knowledge, taught me new things, and, most importantly, inspired me to explore this topic in depth.

I would also like to express my gratitude to my thesis' supervisor, Professor Xiaoshu Lü, for her invaluable guidance, assistance, and support throughout the process of writing this thesis. Your insightful feedback and expertise have been instrumental in shaping this work. I truly appreciate the time and effort you dedicated to helping me succeed.

Finally, I want to thank those who encouraged me, kept me committed to my studies, and supported me throughout the writing process: my family and friends. Above all, I am especially grateful to you, Pontus, for your understanding, inspiration, reassurance, and the morale boost you provided throughout this thesis journey.

Turussa, 4.12.2024

Roosa Kalliovalkama

## Contents

## Figures

## Tables



**Abbreviations**

AWE Alkaline Water Electrolysis

APP Ammonia Production Plant

BESS Battery Energy Storage System(s)

CAPEX Capital Expenditure

$CO_2$ Carbon dioxide

CPV Cryogenic Pressure Vessel

DER Distributed Energy Resource(s)

DNI Direct Normal Irradiance

e.g. For example

ES Energy Storage

ESS Energy Storage System(s)

Fig. Figure

FOM Fixed Operations and Maintenance

GEMS Grid Energy Management Systems

GHI Global Horizontal Irradiation

HRES Hybrid Renewable Energy Source(s)

HVAC High Voltage Alternating Current

HVDC High Voltage Direct Current

IEA International Energy Agency

LCOE Levelized Cost of Electricity

LCOH Levelized Cost of Hydrogen

LHV Lower Heating Value

kg Kilogram(s)

KPIs Key Performance Indicators

KTPA Kiloton Per Annum

kW Kilowatt(s)

kWe Kilowatt Equivalent (electric)

kWh Kilowatt-hour(s)

MSC Minimum State of Charge

MW Megawatt(s)

MWh Megawatt-hour

NREL National Renewable Energy Laboratory (USA)

NTP Standard Temperature and Pressure

OPEX Operational Expenditure

PEM Polymer Electrolyte Membrane

PMT Payment Function

PV Photovoltaic

RE Renewable Energy

RES Renewable Energy Source(s)

SOC State of Charge

TW Terawatt(s)

**Symbols**

$E$ Total Energy [kWh]

$e^-$ Electron

$E_{H_2}$ Energy required to produce one kilogram of hydrogen in kWh

$\eta$ Efficiency expressed in decimals

*(g)* Gass

$H$ Hydrogen Demand [kg]

$H_2$ Hydrogen Molecule

$H^+$ Positive Hydrogen Ion

$H_2O$ Water Molecule

*(l)* Liquid

$P_{eff}$ Effective Power [kW]

$P_{req}$ Power Required [kW]

$O_2$ Oxygen Molecule

$ Dollar (USD)

% Percentage

**Declaration of AI use**

During the writing process of this Master thesis, Roosa Kalliovalkama, the author of the thesis, used artificial intelligence (ChatGPT-4.o) in order to check the spelling, translations, flow, and possible grammatical errors within the text. ChatGPT was only used for proofreading as to assist the author to write the thesis in English, which is not their native language. The author reviewed and edited the contents received from ChatGPT and takes full responsibility for the content of the Master thesis.

# 1 Introduction

Decarbonizing the energy sector is essential for reducing greenhouse gas emissions worldwide (European Commission, 2021). According to the IEA (2023) fossil fuels constitutes for 80% of the global energy supply and are the primary contributors to greenhouse gas emissions, especially when compared to other sectors. With the increasing demand for electricity and regulatory measures from organizations, such as the European Union and the United Nations, aimed at mitigating global warming, industries are required to develop innovative strategies to reduce their emissions and progress towards carbon neutrality, all while accommodating growing energy needs (European Commission, n.d.). This demand creates significant opportunities for the development and deployment of software and hardware solutions within the energy sector.

To explore the role of hybrid hydrogen systems in microgrids and the potential for optimizing its production, utilization, and storage, this research defines key terms and outlines the study's motivation, objectives, and scope. The research questions presented in this section provide a framework for the study, guiding both the research design and the literature review. These questions will also serve as benchmarks for evaluating the study's effectiveness and for clarifying its purpose and significance.

## 1.1 Motive for Research

As of 2017, the majority of hydrogen production has been achieved through steam reforming fossil fuels (Haghi et al., 2017). However, with the shift towards more sustainable energy production methods, researchers are increasing the exploring alternative solutions for hydrogen production (Haghi et al., 2017). One promising method is electrolysis, which has shown immense potential due to its environmentally friendly manner. According to Haghi et al. (2017) , electrolysis uses water ($H_2O$) as the fuel, producing only hydrogen ($H_2$) and oxygen ($O_2$) as byproducts. The electrolysis process, however, does not occur spontaneously; it requires an energy source, which can be nonrenewable,

renewable, or a combination of both (U.S. Department of Energy, n.d.). The use of renewable energy sources (RESs) and distributed energy resources (DERs) significantly supports hydrogen production within microgrids by providing the electrolysis process with a reliable and sustainable energy supply (Shahbazbegian et al., 2023).

Over the last decade, there has been substantial investment in hydrogen production and its storage systems, as hydrogen has long been regarded as the fuel of the future (Sadi & Deymi-Dashtebayaz, 2019). This is one of the driving factors behind the growing body of research focused on optimizing hydrogen systems, with a major focus on hydrogen storage (European Commission, 2024). Hydrogen can be stored in various forms, suited for short-term, seasonal, or long-term applications, and with or without buffering tanks (Kharel & Shabani, 2018). According to Mayyas et al. (2020), utilities and companies using RESs, such as wind and solar, often employ long-term storage systems to capture excess energy from these sources. This stored energy can then be used to stabilize fluctuations in production capacity and to enhance the resilience of power grids as well as the energy mixes (Kharel & Shabani, 2018).

In hybrid renewable energy sources (HRES), it is common for microgrids to generate excess electricity, especially under optimal conditions (Mohammad Amin Vaziri Rad et al., 2023). In microgrids producing hydrogen, this excess energy, also known as surplus power, is directed to the electrolyzer, where water ($H_2O$) is split into hydrogen ($H_2$) and oxygen ($O_2$) molecules (Haghi et al., 2017). The hydrogen produced by excess electricity is then stored in either liquid or gaseous form under high pressure. Depending on the storage system, the stored hydrogen can be used immediately, sold to industries or electrical utilities, or stored for later use (Kharel & Shabani, 2018). The hydrogen can be distributed through $H_2$-pipelines, while excess electricity can be transmitted through traditional high voltage alternating current (HVAC) or high voltage direct current (HVDC) grids (Mancarella, 2021) (Figure (Fig.) 1).

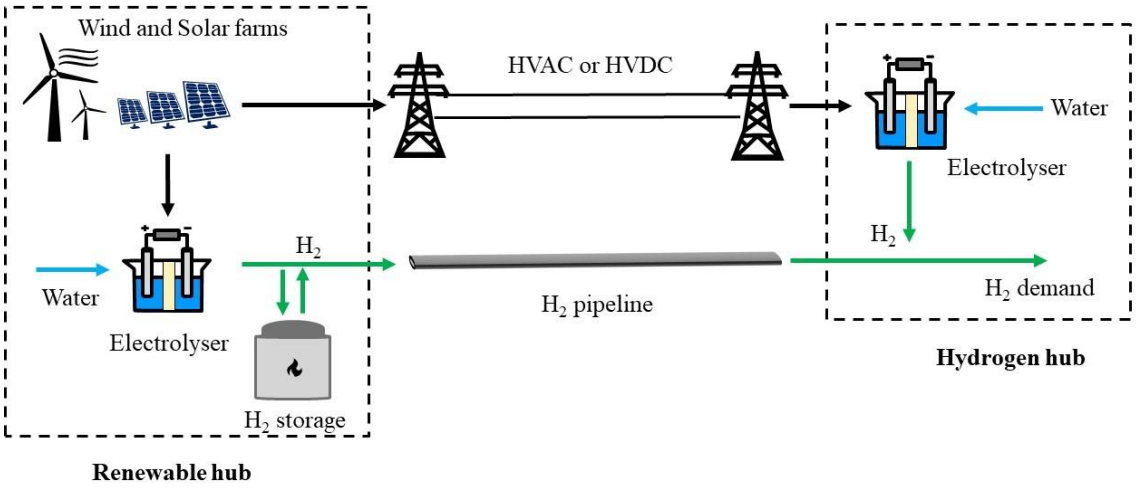


**Figure 1**. Sketch of a renewables-hydrogen hybrid corridor (Mancarella, 2021).

The Levelized Costs of Electricity (LCOE) and Hydrogen (LCOH) are influenced by multiple factors. According to Directorate General for Energy (European Commission) et al. (2020) some factors, which influence the LCOE and LCOH values, are the Capital Expenditure (CAPEX) and Fixed Operation and Maintenance (FOM) costs of the used technologies, the locations' resources and their capacity factors, and financial factors, like the discounts and Weighted Average Cost of Capital (WACC). This thesis aims to reduce the chosen Key Performance Indicators (KPIs) values by determining component capacities through the application of a *Trial-and-Test Method*, thereby lowering both the CAPEX and FOM associated with the case study microgrids.

## 1.2 The Objective and the Scope

The aim of this research is to analyze the cost-economic factors of hybrid hydrogen systems in microgrids and assess their feasibilities through *Test-and-Trial* processes. The focus is on minimizing the LCOE and LCOH, while minimizing the excess electricity generation. This entails maximizing renewable energy (RE) output, enhancing efficiency of

microgrid component capacities, and addressing system requirements, constraints, and generation asset limitations. The research also seeks to balance RE and component sizing to meet hydrogen and electricity demands within an independent, or in islanded, microgrid under different scenarios. Additionally, the study addresses the stabilization of RE output fluctuations by leveraging hydrogen and electrical storage systems to meet the load demands of the microgrid.

The objective of this research is to evaluate the techno-economic costs associated with hybrid hydrogen systems by developing case study models and analyzing the impacts of fluctuating RESs and varying load profiles. Specific case studies will be introduced in subsequent sections of the thesis. This research aims to design models for future microgrid applications that incorporate the utilization of electrolyzers, wind turbines, solar panels, hydrogen storage, battery systems, and other essential microgrid components. These models are intended to facilitate customized solutions for companies on a global scale.

The research questions are designed as clear inquiries that identify the key aspects of microgrid modelling to be examined, providing focused direction for the project. The research questions for this thesis are as follows:

1. How do distinct locations and running profiles impact the performance and costs of the microgrid system?
2. What are the interdependencies between component capacities in the case studies presented in this thesis?
3. What scenarios, locations, and climates, support the cost-effective hydrogen production and systems?

# 2 Literature Review

Currently, there is limited publicly available research on methods of hydrogen production, utilization, and storage in industrial-scale operations. Nonetheless, selection of articles, both publicly accessible and restricted, offers valuable insights that support the development of simulation models for hydrogen-producing microgrids.

## 2.1 The Color Codes of Hydrogen

Hydrogen types are generally classified into color-coded categories based on the production method, with particular attention to the energy source and associated emissions (Ziętek, 2022). There are nine recognized hydrogen color groups: *Grey*, *Blue*, *Turquoise*, *Green, Black/Brown, White, Red, Purple and Pink Hydrogen* (Hydrogen Europe, n.d.). Among these, the *Grey, Blue*, and *Green* categories are the most relevant to this research, particularly from the perspective of decarbonization, which is a central theme of this thesis. Hydrogen can be produced through multiple different processes with either renewable or nonrenewable sources (Kumar & Lim, 2022). Due to the decarbonization of the energy sector, the trend has been to produce more and more hydrogen with RESs, HRES, and other carbon neutral sources, like sustainable fuels (Kumar & Lim, 2022).

*Grey Hydrogen* refers to hydrogen produced through the steam reforming of hydrocarbons (Hydrogen Europe, n.d.). This production method is categorized as a high carbon dioxide ($CO_2$) emitter, with emissions estimated to be between 9 and 12 kilograms of $CO_2$ per kilogram of hydrogen (Hydrogen Europe, n.d.). Despite its high efficiency and resource sufficiency, the use of *Grey Hydrogen* is controversial due to its significant environmental impact (Hydrogen Europe, n.d.). For this reason, producing hydrogen in this manner is deemed unacceptable for the purposes of this research, which focuses on decarbonization.

*Blue Hydrogen* refers to hydrogen produced from fossil fuels, with carbon capture technologies employed during the process to reduce emissions (Hydrogen Europe, n.d.). While this method is classified as a low $CO_2$ emitter, due to the capture of $CO_2$ during production, it is important to consider the entire life cycle of *Blue Hydrogen* production (Hydrogen Europe, n.d.). According to Hydrogen Europe (n.d.), when the full life cycle is accounted for, this method can result in higher emissions than the actual usage of the fossil fuels themselves. Since this thesis considers the entire life cycle of hydrogen production and aims for a carbon-neutral outcome, *Blue Hydrogen* is deemed unsuitable for this research.

*Green Hydrogen* refers to hydrogen, most often, produced by water electrolysis, by using renewable energy sources (RESs) (Hydrogen Europe, n.d.). The water electrolysis process is explained in the next segment of this chapter, and thus not further opened here. *Green Hydrogen* production and usage of this method is $CO_2$ emission free (Hydrogen Europe, n.d.). This coupled with the fact that the method utilizes only RESs as a source of energy, ***Green Hydrogen* is suitable as the group of hydrogen used within this thesis' research.**

## 2.2 Water Electrolysis

Water electrolysis is a chemical process in which water, when exposed to an electrical current, undergoes a reaction to produce hydrogen and oxygen (Millet & Grigoriev, 2013). As written above, for hydrogen produced through this process to be classified as *green*, the electricity used must come from RESs with minimal emissions, such as low-carbon sources (Kumar & Lim, 2022). As for 2020, however, 95% of hydrogen is produced with nonrenewable energy sources, primarily due to the high cost of green hydrogen production (Mosca et al., 2020).

Electrolysis is an electrochemical reaction, where anode and cathode are driven to react based on their electrochemical properties, such as potential differences (Wang et al., 2014). In water electrolysis, fresh water, electricity, and sometimes heat are used to

produce hydrogen and oxygen (Kumar & Lim, 2022). The reaction happens in an electrolyzer, a device consisting of an anode, cathode, and electrolyte (U.S. Department of Energy, n.d.). While electrolyzers vary in function, size, and component materials, they share a similar fundamental mechanism (David et al., 2019) (see Fig. 2). Two different electrolyzer types are further explored in chapter *3.2. Different Water Electrolyzers.*

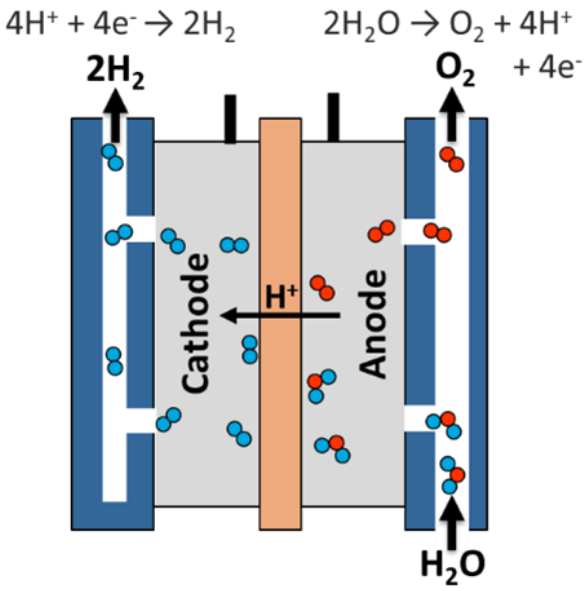


**Figure 2.** The basic structure and process of electrolyzer (U.S. Department of Energy, n.d.)

According to Zumdahl & Zumdahl (2000, p. 864-865), the core function of an electrolytic cell is to use electrical energy to drive a nonspontaneous chemical change, transforming reactants into products. In water electrolysis, this process forces water molecules to decompose, producing hydrogen and oxygen (Zumdahl & Zumdahl, 2000, p. 866-867). Under standard temperature and pressure condition (NTP-condition), electrolysis is an endothermic and nonspontaneous reaction (Millet & Grigoriev, 2013). The balanced equation for this reaction is shown below (Equation 1), and in it water splits into hydrogen and oxygen.

The water electrolysis reaction

$$2H_2O\ (l) \rightarrow 2H_2\ (g) + \ O_2\ (g), \qquad (1)$$

where $H_2O$ is water, $H_2$ is hydrogen, and $O_2$ is oxygen molecule.

In addition to the main reaction, there are distinct reactions occurring at each electrode. When an electrical current passes through interconnected electrolysis cells (or stacks) to the anode (negative electrode), water molecules decompose to form positively charged hydrogen ions and oxygen molecules (U.S. Department of Energy, n.d.). The hydrogen ions then move through the electrolyte, electrons flow through an external circuit, and oxygen is released unless otherwise utilized (U.S. Department of Energy, n.d.). The reaction occurring at the anode is presented below (Equation 2).

The reaction to anode in water electrolysis is

$$2H_2O\ \rightarrow\ O_2 + 4H^+ + 4e^-, \qquad (1)$$

where $H^+$ is positive hydrogen ion and $e^-$ is electron.

The second reaction occurs at the cathode side (positive electrode). Here the hydrogen ions and electrons, now oppositely charged, combine into hydrogen gas molecules (U.S. Department of Energy, n.d.). Unlike the anode reaction, the cathode reaction is spontaneous and does not require energy input (U.S. Department of Energy, n.d.). Once generated, the hydrogen can be stored or utilized as needed. The cathodic reaction is shown below (Equation 3).

The reaction to anode in water electrolysis is

$$4H^+ + 4e^- \rightarrow 2H_2\ , \qquad (2)$$

where $H^+$ is positive hydrogen ion, $e^-$ is electron, and $H_2$ is hydrogen molecule.

For the water electrolysis to proceed under NTP-conditions, the process requires an initial input energy, known as activation energy (Millet, P. & Grigoriev, S., 2013, p. 20). The

activation energy break the chemical bonds within water molecules, while overpotential is required to drive the reaction regardless resistance (Millet & Grigoriev, 2013, p. 20). Thermodynamic factors, like the Gibbs energy, enthalpy, and entropy, are also critical while assessing the feasibility of the reaction (Millet & Grigoriev, 2013, p. 22). Due to the overpotential and ohmic loss of the system, the actual voltage required for water electrolysis is in reality higher than theoretical voltage (Millet & Grigoriev, 2013, p. 22).

## 2.3 Different Water Electrolyzers

The basic function of the electrolyzer, whether the electrolyzer is polymer electrolyte membrane (PEM), alkaline (AWE), or solid oxide electrolyzer, is similar, with all three options currently suited for common usage (Kumar & Lim, 2022). However, emerging technologies are likely to alter this landscape in the near future. These three options are often suited for usage nowadays, but there are new technologies which will most likely change this setting (Kumar & Lim, 2022). These technologies all have advantages and disadvantages. Selecting one of them, factors such as conversion efficiency, CAPEX requirements, and application requirements, like load profile and fluctuations within the microgrid, must considered (IEA, n.d.). This section provides a focused comparison between PEM and AWE electrolyzers, as these technologies are relatively mature and offer several advantages (Ayers, 2019; David et al., 2019; Hu et al., 2022).

The electrolyzers efficiency is influenced by its material and properties, the conditions of the electrolysis, and many other factors (Millet & Grigoriev, 2013). For instance, PEM and AWE electrolyzers differ significantly in terms of CAPEX and electrical efficiency. As of 2019, the CAPEX for AWE ranged between 500–1400 $/kWe with an electrical efficiency of 63–70% (LHV), while PEM systems had a CAPEX of 1100–1800 $/kWe and an electrical efficiency of 56–63% (LHV) (IEA, 2019). This research focuses primarily on their performance under intermittent conditions. Fluctuations in energy from sources like wind and solar are often inevitable, as they are strongly influenced by location and weather conditions (Kojima et al., 2023, p. 4574).

The restrictions of water electrolyzers' operating conditions, compatibility, and performance under the fluctuating energy have not been evaluated nor investigated thoroughly (Kojima et al., 2023, p. 4587). While PEM and AWE electrolyzers both respond similarly to energy fluctuations, these fluctuations negatively impact electrolyzer operation by altering electrolysis conditions, such as pressure and temperature, which can disrupt process stability (Kojima et al., 2023, p. 4587; Nasser et al., 2022, p. 87002). The intermittent of RESs causes the electrolyzer to operate outside of the optimal operation, affecting their efficiency, stability, and increasing the potential of damage within them, like the degradation of the catalysts, which is the main cause of degradation in an electrolyzer (Kojima et al., 2023, p. 4577). The stress on the equipment is further increased by the number of start-ups and shut-downs, also affecting the stability of real-time processing, lifetime, and durability of the electrolyzer (Kojima et al., 2023, p. 4577; Nasser et al., 2022, p. 87012-87013).

According to Kojima et al. (2023, p. 4587), especially AWE electrolyzers are affected by the catalyst degradation of the reverse current in start and stop operations. Another constrain of AWEs are that under a low power loads they are not effective, even though they are rather safe to be used under a non-stop fluctuating power operation (Kojima et al., 2023, p. 4587). PEM electrolyzers, however, are not as vulnerable to the degradation of its catalysts and can operate well with the fluctuating energy sources and under low load power (Kojima et al., 2023, p. 4587). As written before, PEM's investment cost is significantly higher than AWE's, due to the noble metal catalysts. To reduce costs, the catalysts need to be developed with only the necessary amount of noble metals, ensuring that neither the lifetime nor performance of the PEM electrolyzer is compromised (Kojima et al., 2023, p. 4587). While significant development is needed for both PEM and AWE technologies, the PEM electrolyzer is currently the better-suited option for modeling a microgrid system of this size.

## 2.4 LCOE and LCOH Calculations with PMT-Function

The calculation of LCOE and LCOH values ensures that the cost metrics accurately represent the unique system architectures and the application of the *Trial-and-Test Method* for each model, thereby providing a robust foundation for further analysis. The recalculated LCOE and LCOH values are derived using Excel's PMT-function (Payment function), which calculates loan payments based on constant payments and interest rates (Microsoft Support, n.d.). The detailed calculation processes are explained below, using parameters from Appendix 3.

The calculation begins with the LCOE, which is needed to calculate the LCOH, as the LCOE serves as "the price of fuel" in the LCOH calculation. After this, the LCOH in dollars per megawatt-hours ($/MWh) is calculated, as it is then required to calculate the LCOH in dollars per kilograms ($/kg). The LCOE calculation starts by determining the annual generation of all components. This is done by multiplying each component's capacity, capacity factor, and the system's operating hours, which is 8,760 hours per year. The *Annual Power Generation* is the sum of wind and solar generation, while the *Annual Hydrogen Generation* is based on the electrolyzer's output. The *Annual Hydrogen Generation* is excluded when calculating the LCOE but included in the LCOH calculation.

The LCOE is calculated by summing the LCOEs, which include both CAPEX and FOM, of all electricity-generating components, such as wind turbines, photovoltaic (PV) panels, converters, and battery energy storage system (BESS). These calculations use the PMT-function. The required inputs for the PMT-function are the Weighted Average Cost of Capital (WACC) in percentages (%), the component's economic life (years), CAPEX or FOM ($/kW, for electrolyzer $/kg), the component's capacity in megawatts (MW), and Annual Power Generation in megawatt-hours (MWh). Once collected, these parameters are entered into the functions (5 & 6) in Excel, in order to calculate the LCOE with the CAPEX and FOM costs.

The PMT-function is for the PV panel's is

$$PMT(WACC, Economical\ Life_{PV}, \frac{-CAPEX_{PV} * Capacity_{PV} * 1000}{Annual\ Power\ Generation}, \quad (3)$$

where the parameters are those of PV panel.

If the PMT-function is used to calculate the LCOE with FOM, the only difference to change within the function above is to change the CAPEX to the FOM cost value (Appendix 2). Once the LCOEs of all components, including both CAPEX and FOM costs, are calculated separately, these values are summed to obtain the total LCOE for the system in each specific case study. After the LCOE values for all nine case studies are calculated, they are used in the calculation of the LCOH values.

The LCOH ($/MWh) is calculated similarly to the LCOE, with the exception of the *Electricity Cost*, which is one of the values summed together in order to calculate the LCOH of the system. The Electricity Cost is calculated by dividing the system LCOE (in table above) with the electrolyzer's efficiencies, which differ between the case studies. The other two values, summed with the *Electricity Cost*, are the LCOH values for electrolyzer, as this component is the only component used to generate hydrogen, due to the exclusion of hydrogen tank. The LCOH ($/MWh) values for electrolyzer are calculated with the equation (5) below.

The PMT-function is for the calculation LCOH ($/MWh) is

$$PMT(WACC, Economical\ Life_{PV}, \frac{-CAPEX_{Elect.} * Capacity_{Elect.} * 1000}{Annual\ Hydrogen\ Generation}, \quad (4)$$

where the parameters are those of electrolyzer's.

If the PMT-function is used to calculate the LCOH ($/MWh) with FOM included, the only adjustment required is to replace the CAPEX value with the FOM cost (Appendix 2), as when calculating the LCOE values (Appendix 3). Once the LCOH values, including both CAPEX and FOM costs, are calculated alongside the *Electricity Costs*, they are summed to obtain each case study system's overall LCOH ($/MWh) value.

The final step in calculating LCOE and LCOH values is to determine the LCOH ($/kg) by dividing the LCOH ($/MWh) by the energy content of hydrogen (the lower heating value or LVH), which is 33.3 MWh/kg.

## 2.5 Hydrogen Energy Storage Systems

Energy storage (ES) is essential to microgrids that rely on RESs due to their inherent intermittency and variability (Kharel & Shabani, 2018). To mitigate the unreliability of RESs, innovations such as Grid Energy Management Systems (GEMS) and various energy storage solutions have been integrated into microgrid designs (Kharel & Shabani, 2018). This research focuses on two specific types of storage relevant to the case study scope: electrical storage (batteries) and hydrogen storage. While there are numerous forms of both short- and long-term storage, this research narrows its focus to those applicable in microgrids and compatible with RESs. According to Jayawardana et al. (2019) energy sources, like the solar PV and wind, are vulnerable to inconsistent sources of energy, thus some kind of a storing device is highly recommended.

The process of converting excess electricity into hydrogen for storage and later use, known as *Power-to-Hydrogen* or *Power-to-Gas*, offers a valuable approach for balancing RESs (Götz, 2016). In 2024, the primary storages for hydrogen are the physical and chemical hydrogen storages (Ma et al., 2024). Among physical storage methods, compressed, liquified, adsorbed, and cryogenic compressed hydrogen are prevalent, while chemical storage includes metal hydrides and fuel cells (Götz, 2016; Ma et al., 2024). For this research the most interesting are the pressurized storage vessels, especially in cryogenic hydrogen storage systems. According to Moreno-Blanco, J., Petitpas, G., et al. (2019) these cryogenic pressure vessels (CPVs) utilize high pressure inner vessel, an outer metallic vacuum jacket, and a vacuum space between these two. Because of the outer vacuum jacket, which creates a second layer of protection to the vessel, the cryogenic storage vessel is less exposed to environmental impacts (He et al., 2021).

In addition to the safety aspects of CPVs, the density of stored hydrogen is significantly high as it the hydrogen is stored under high pressure and at low temperature in a liquefied state (Aceves, S., M., et al., 2013). With the ability to work at a pressure of 350 bars and at a temperature of 20 K, the CPVs are compact, cost effective, safe, and enhanced (Aceves, S., M., et al., 2013). Compared to other hydrogen storage vessels, cryogenic compressed hydrogen storage is particularly suitable for microgrid applications, where rapid and frequent release and storage of hydrogen may be necessary (Aceves, S., M., et al., 2013).

# 3 Research Methodology

The research methodology of this thesis entails developing multiple models through utilization of *Trial-and-Test Method* when using HOMER Pro software. This process includes data collection, constructing simulation models in HOMER Pro, researching the relations of the component capacities through the *Trial-and-Test* process and subsequently analyzing and comparing simulation results.

## 3.1 HOMER Pro -software

HOMER Pro is a globally standardized software tool used for optimizing microgrid designs across various microgrid applications (HOMER Pro Software, n.d.). The software enables simulation, optimization, and sensitivity analysis of the selected grid configurations. Depending on the system setup and equipment, HOMER Pro simulates all possible combinations, even if there are hundreds or thousands of configurations, in a single simulation run (HOMER Energy, n.d.-h). The simulation can model grid operations for an entire year, with time steps ranging from one minute to one hour, depending on the preferences for the simulated system. After running the simulations, users can instruct HOMER Pro to sort the results based on the chosen variables (HOMER Energy, n.d.-h).

There are additional modules, which can be integrated into the simulated systems to add powerful modelling capabilities e.g. multiple variables of HRESs (HOMER Energy, n.d.-g). In this research, the module which is the most intriguing is, the *Hydrogen Module*. This module allows the user to simulate, optimize, and analyze sensitivity of their model and its systems, which produce, consume, or otherwise utilize hydrogen in it (HOMER Energy, n.d.-f). The HOMER Pro website portrays the hydrogen module as follows:

> It is ideal for users who model fuel cells, remote off-grid operations, large industrial processes, or any system with hydrogen production, storage, or consumption. This module adds a reformer, electrolyzer, and hydrogen tank components [*sic*]. It also adds a hydrogen load and stored hydrogen fueled generator. (HOMER Energy, n.d.-f).

Academic institutions, industries, and companies worldwide use HOMER Pro to simulate their projects (HOMER Energy, n.d.-i). The choice to use this software in this research for simulating the usage and production of hydrogen within a microgrid is based on its ability to simulate thousands of variables, identify the most cost-effective options, compare results, and analyze the impact of variables beyond my control. Additionally, the inclusion of the *Hydrogen Module* makes it particularly well-suited for this study.

## 3.2 Data Collection

This research study draws on data collected from scientific literature, HOMER Pro guides and simulations, as well as discussions with experts in decarbonization, sustainability, and business. The scope of the research is focused on the most desired component sizing, cost efficiency, and performance under varying conditions. Emphasis is placed on identifying configurations that balance operational feasibility with environmental impact, aiming to support scalable, region-specific applications in line with carbon neutrality goals.

## 3.3 The Study of the Microgrid

This section introduces the microgrid, its components, and layout to provide a detailed understanding of the motivations and objectives behind this thesis. The information is informed by discussions, interviews, and consultations with decarbonization specialists. Key input elements required to build the microgrid models, including RESs and industry inputs, are outlined below, while Fig. 3 illustrates the scope of the microgrid models.

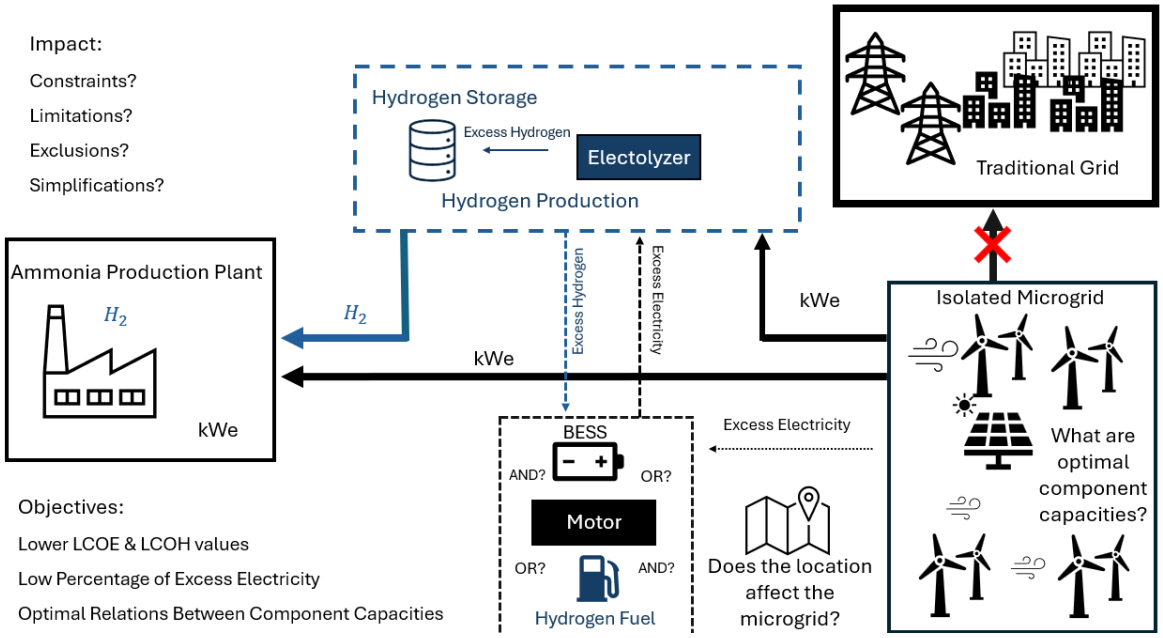


**Figure 3.** Scope of the Microgrid.

This methodology aims to create a structured approach for this research, particularly for the development and refinement of the case study models. Fig. 3 highlights the boundaries, focus areas, objectives, and essential elements within the microgrid models explored in this thesis. These models prioritize simulating selected case studies under various parameter conditions, integrating and analyzing components and capacities, assessing feasibility, exploring potential constraints, minimizing the KPIs, and evaluating results to determine the need for further study.

### 3.3.1 Load Profile

The term load profile can be applied in various contexts. In this research, it refers specifically to electricity usage. According to Mugo, (2022) the load profile is " the approximate energy required by a system over a specific period" (Mugo, 2022). Load profile often includes details on how and for what purposes energy is used. For example, it may refer to data consumed or demanded energy and is typically presented either as a dataset or as a graph (Elexon UK, 2022). Energy consumption and demand are essential factors

when optimizing power systems such as microgrids. Mugo (2022) identifies two methods for calculating the power load profile: the *24-Hour Method* and the *Autonomy Method*.

### 3.3.2 Exclusions on the Setup and in Load Profile

As previously mentioned, microgrids in case studies operate in islanded mode, producing electricity and hydrogen to meet the demand of an industrial size ammonia production plant (APP), as detailed in Appendix 1. The decision to operate the microgrid in islanded mode was made to narrow the research scope by excluding factors related to the main grid, such as tariffs, environmental impacts of energy sources, and frequency and voltage regulations. Including these factors would expand the focus beyond the goals of this thesis, so they have been deliberately omitted. Future research could explore grid-connected scenarios for additional insights.

In line with the decision to focus on the microgrid, the APP's processes and end-products are intentionally excluded from this study. The focus is solely on the plant's electricity and hydrogen load profiles, without considering other operational aspects of the plant. The primary objective is to support the production of $CO_2$-free products that meet end-user demands, supplied by the microgrid. However, there are constraints on the hydrogen and electricity produced by the microgrid: both must be generated exclusively from RESs.

The load profiles for both electricity and hydrogen are maintained as constant during the operating hours of the APP. These variations are predefined and established at the beginning of each case study model simulation. Detailed descriptions of the case studies are provided in chapter 7, *Case Studies*.

### 3.3.3 The Components of Microgrid

To meet the demand of electricity and hydrogen for the APP, the microgrid models in this study include several components: wind turbines, solar panels, batteries, hydrogen tanks, electrolyzers, and converters. Wind turbines and solar panels generate electricity, batteries store excess energy, electrolyzers produce hydrogen, hydrogen tanks store surplus hydrogen, and converters manage the conversion between alternating (AC) and direct currents (DC) buses. These components are integrated into microgrid models to accurately simulate the operational environment for the study cases.

According to Žigman et al. (2024), in islanded mode the microgrid components tend to be 'substantially larger' to meet the load profile. This implies that the system must be equipped with high-capacity components or a larger number of components to achieve the required total capacity. Since the size and quantity of these components directly influence the overall system costs, examining their relationships is a central focus of this study. This analysis is conducted using the *Trial-and-Test Method*, which is described in detail later in the thesis.

While each component in the microgrid has a specific function, its performance also contributes to the overall system's efficiency and synergy. For example, determining the electrolyzer’s capacity involves balancing factors such as hydrogen demand, use of RESs, integrating with other microgrid components, and mitigating the effects of RES intermittency (Muyeen et al., 2019, p. 221). Although several types of electrolyzers are available, due to some simplifications made during the model simulation process, only generic components were used within the simulation models. Further explanations for simplifications are in *Discussion* chapter.

## 3.4 Trial-and-Test Method

The case study models simulation process follows the *Trial-and-Test* Method approach, a process where the configurations and parameters of microgrid systems are continuously refined to achieve desirable solutions for this research, culminating in a model adaptable to various scenarios (Gupta, 2022). This process begins by defining the goals for the *Trial-and-Test Method* and its process, which are:

1. To meet the hydrogen and electricity demand in all nine case study load profiles.
2. To achieve the most favorable models possible using the *Trial-and-Test* process on case study models.
3. To analyze the cost impacts of the different components both within and across the case studies.

The *Trial-and-Test* is an approach aimed at continually improving the creation of the model's design (Gupta, 2022). The modeling process starts with the creation of the base set-up which is incrementally modified through multiple simulation runs. Each simulation run adjusts parameters or components to decrease the KPI values of that model's results. The *Trial-and-Test* process refines the requirements for the model while identifying the synergies and their results within the microgrid models. According to Branch (n.d.), this process relies on sequential steps and provides flexibility to quickly incorporate changes, involving continuous planning, analysis, implementation, and evaluation of prototype models throughout the simulation processes of the models.

The *Trial-and-Test* process was selected as the research method after reviewing information on the islanded microgrid and the APP (see Appendix 1). While the components to be integrated into the models are known, specific parameters and variable inputs remain uncertain. The aim of this research was to analyze green hybrid hydrogen systems across nine case study scenarios and to compare variations in location and operating profiles.

# 4 Modelling in HOMER Pro

In this chapter, a model is created in HOMER Pro with the primary objective is to study the modeling tool. While designing the model, it is essential to consider not only the specific components of the microgrid but also the load requirements and the available resources for the selected ESs. The case study models focus on an industrial-scale, islanded microgrid designed to provide both electricity and hydrogen to customers. For this practice model, the components and resources are configured with basic settings, primarily using predefined parameters provided by HOMER Pro. The exception is the load parameters, which are customized based on inputs from Appendix 1. The location chosen for the practice model is in northern Tasmania, selected due to its abundant wind and solar resources.

Figures included in this chapter are screenshots of the simulated model from HOMER Pro. The software version used is HOMER Pro Microgrid Analysis Tool x64 3.18.0. The figure below (Fig. 4) shows the *Home page* of the software, where users can define basic inputs such as the project's name, author, and location, as well as more detailed settings such as the project's lifetime and inflation rate. Precise input settings are critical, as even minor inaccuracies can significantly affect simulation results. Similarly, a clear understanding of the component parameter configurations is vital for ensuring accurate modeling; these configurations are briefly described below.

The basic design of the modeled microgrid aligns with the scope introduced earlier in this thesis (see Fig. 3). Advanced parameters of the components remain unexplained, as most of them remain unedited for the case studies.

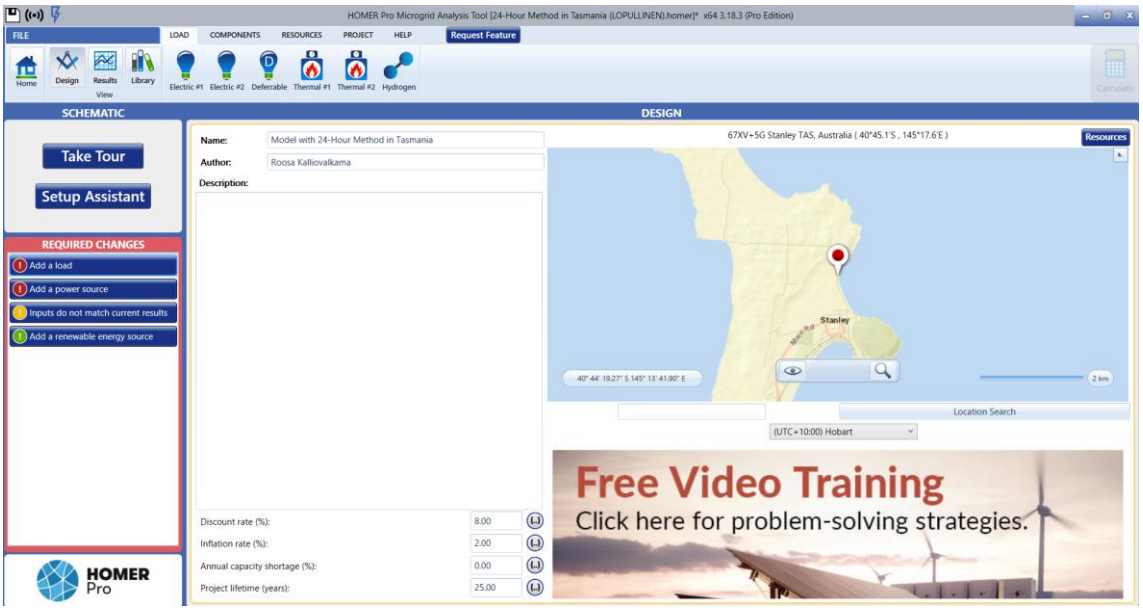


**Figure 4.** Home page of HOMER Pro.

## 4.1 The Load Profiles

Modelling a microgrid commences with the load side of the system, as the design, sizing, and operation of all other components are determined by the demand (HOMER Energy, n.d.-q). According to HOMER Energy (n.d.-g), the load represents the portion of the system that consumes energy, excluding losses within the system. Load setup involves multiple critical parameters that influence the model's layout, component sizing, cost-effectiveness, and overall performance. Defining and setting both electrical and hydrogen load parameters in the model is essential for ensuring the simulations reflect real-world conditions. By adjusting these parameters, users can explore various scenarios, determine system configurations, and evaluate results in terms of financial, economic, and environmental impacts, all while meeting load demands under different conditions.

The electrical and hydrogen load inputs are illustrated in Appendix 1. The load profile is based on an APP, which has a consistent industrial profile without peak months and

annually operates for 8,000 hours. According to HOMER Energy (n.d.-f), hydrogen load refers to the external demand for hydrogen, which, in this simulation, represents the demand of the APP.

In contrast, the electrical load represents external electricity demand, which includes the power needed for electrolysis but excludes the microgrid's internal energy consumption. Microgrids require power for their own systems, but this internal demand is excluded in the defined load (HOMER Energy, n.d.-p).

The profiles for both electrical and hydrogen loads are shown below (see Fig. 5 and Fig. 6). The metrics are based on an average electrical load of 30 MW and a hydrogen load of approximately 5,822 kg per hour, with a load factor of 0.55. The APP operates continuously, 24 hours per day, following the *24-Hour Method*. These load profiles are applied to all three case study models using the *24-Hour Method*, which will be introduced in subsequent sections of this thesis.

### 4.1.1 The Electric Load

According to HOMER Energy (n.d.-g), the load is a part of the system that consumes energy, excluding any potential system losses. Setting up the electrical load in HOMER Pro requires configuring parameters essential for simulating the microgrid as a whole. Some load parameters have to be specified in HOMER Pro prior to inclusion in the model, while others are configured post-addition. As shown in Fig. 7, these electrical load parameters include the simulation year, random variability (day-to-day and timestep percentage differences), advanced efficiency settings, load type (AC or DC), and the scaled annual average kilowatts per day (HOMER Energy, n.d.-j). Brief explanations of these parameters are provided to underscore their importance in the microgrid modeling process. Electrical load parameters play a critical role in determining the model's layout, component sizing, cost-effectiveness, and overall success.

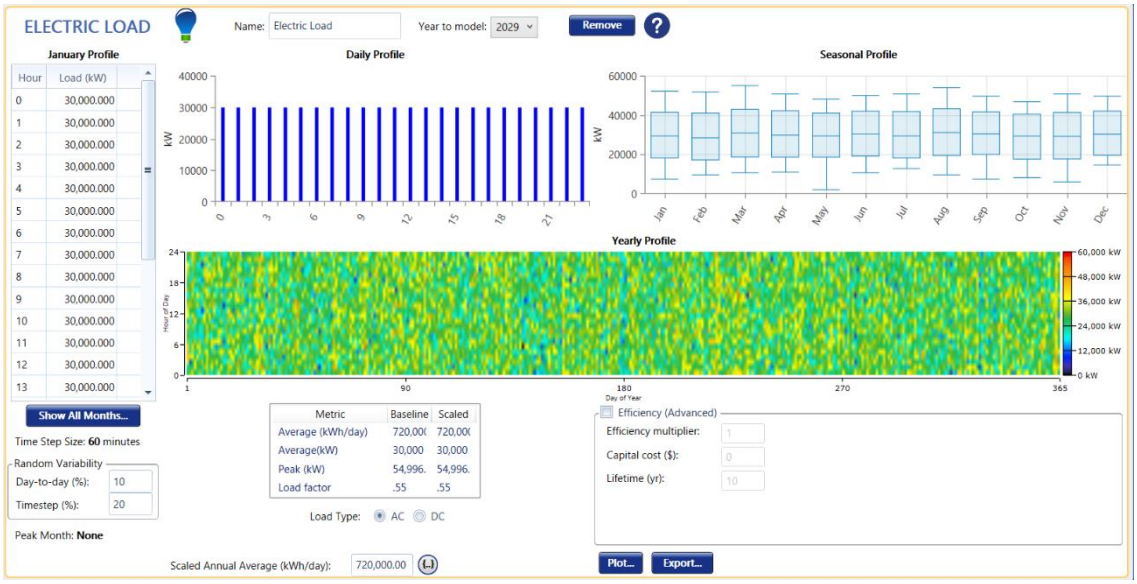


**Figure 5**. Electrical Load Setup for the *24-Hour Method*.

The selected simulation year influences load dynamics due to shifts in weather patterns and varying energy demand, which can be affected by factors such as economic conditions and user behaviors. Including parameters for random variability is essential for generating realistic load profiles, with some variability pre-set in the simulations, though manual adjustments are necessary for a complete day-to-day approximation. Advanced efficiency parameters impact system performance, influencing reliability, optimal usage, and component sizing requirements (HOMER Energy, n.d.-z). The load type (AC or DC) affects compatibility with RESs and may necessitate additional components, such as converters, which must account for conversion losses. The scaled annual average kW/day aids in estimating component sizing, supporting cost-effective system design (Lambert, 2006).

### 4.1.2 The Hydrogen Load

According to HOMER Energy (n.d.-f), the hydrogen load represents the external demand for hydrogen. Similar to the electrical load, setting up the hydrogen load involves multiple parameters, most mirror those used for the electrical load (Fig. 8). The primary

differences are the units, such as kilograms per day ($/kg) for hydrogen versus kilowatts per day (kW/day) for electricity, and a few hydrogen-specific parameters. The *Hydrogen Parameters* include the maximum unmet hydrogen load percentage, the unmet hydrogen load penalty ($/kg), and the value of electricity in dollars per kilowatt-hours ($/kWh). These parameters can be imported from a file or manually entered. While many parameters are similar to those for the electrical load, this section focuses only on those specific to hydrogen, as their role in defining the demand, quantity, timing, and constraints is crucial to the hydrogen load and its broader system.

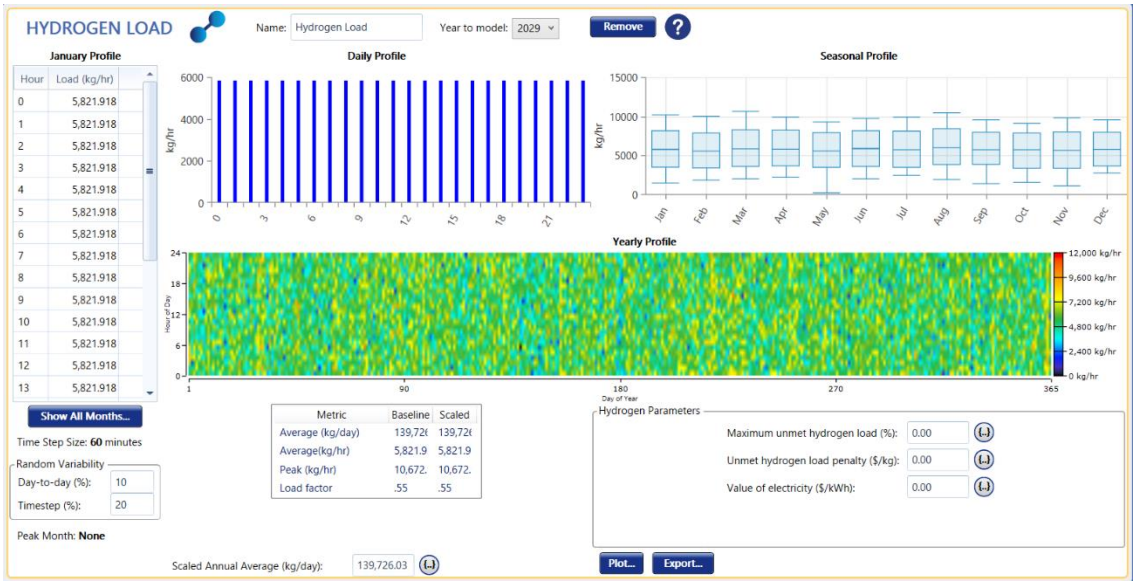


**Figure 6**. Hydrogen Load Setup for the *24-Hour Method*.

The maximum unmet percentage of the hydrogen load establishes the allowable shortfall in meeting the hydrogen demand (HOMER Energy, n.d.-x). The unmet hydrogen load penalty represents the financial penalty for failing to meet hydrogen demand, measured in $/kg. This parameter incentivizes the system to minimize unmet demand by imposing a financial cost, thereby encouraging reliability and efficiency.

The value of electricity determines the cost of electricity ($/kWh) used or generated within the microgrid (HOMER Energy, n.d.-y). This parameter is essential for system cost calculations and deriving the LCOH, a KPI in this thesis. The value of electricity is directly

tied to the cost-effectiveness of hydrogen production and impacts the economic feasibility analysis.

## 4.2 Resources

According to HOMER Energy (n.d.-h), resources such as solar radiation and wind speed are essential inputs for energy modeling. This data can be sourced from the internet, time series data files, or a user's library. HOMER Pro enhances modeling accuracy by capturing detailed information about intermittent RE sources at hourly intervals, enabling precise simulations and forecasting (Lambert, 2006). In HOMER Pro, the *Solar Global Horizontal Irradiance* (GHI) and *Wind* resource tabs (illustrated in Fig. 7 and 8) are used to enter the data from *Renewables.ninja*, which provides hourly wind speed and solar radiation data that must be processed and formatted correctly before being imported into the software.

During prototype simulations, it became apparent that the wind and solar resource capacity factors calculated in HOMER Pro differed significantly from those displayed on *Renewables.ninja*. The capacity factor, a critical metric influencing resource input accuracy, is essential for realistic energy modeling. After selecting the location and viewing the resource capacity factors on *Renewables.ninja*, HOMER Pro simulations produced inconsistent results.

To address this issue, the wind and solar resource data files were scaled before being imported into HOMER Pro. This adjustment ensured the capacity factors in the model aligned with those from the source website, maintaining consistency and improving the validity of the results. Detailed explanations of the scaling process, specific to each case study model, will be discussed in later sections of this thesis.

### 4.2.1 Solar GHI Resource

The use of GHI instead of *Direct Normal Irradiance* (DNI) as a solar resource in this simulation is based on the ability of flat PV panels to capture direct, diffused, and reflected radiation (HOMER Energy, n.d.-u). When downloading the solar radiation input file from *Renewables.ninja*, the direct and diffuse irradiance values are combined to create the required format for the solar input file. GHI's ability to account for indirect radiation expands its scope for capturing solar energy. However, if the case study systems were optimized for direct solar radiation, DNI would be a more suitable option (Madhlopa, 2022).

In this section, the parameters of the GHI solar resource imported from *Renewables.ninja*, are briefly explained, as they are used in the case studies. The downloaded parameters for the GHI resource include the monthly average clearness index and daily radiation (HOMER Energy, n.d.-u).


**Figure 7.** Solar GHI Resource for Tasmania.

According to HOMER Energy (n.d.-a), the clearness index measures the atmosphere's condition, indicating whether the sky is cloudy or clear. Since the clearness of the atmosphere influences the amount of solar radiation reaching the Earth's surface, this factor

is critical in simulations (HOMER Energy, n.d.-a). A higher clearness index indicates a cleaner atmosphere, reducing the atmospheric effect on the radiation (See Fig. 7). The monthly average radiation per day is calculated by summing the daily radiation over the number of days in the month. These values for clearness index and average monthly radiation are presented both in a table and a graph (See Fig. 9). Using these two parameters, HOMER Pro calculates the scaled annual average solar radiation for the location in terms of kWh/m²/day (HOMER Energy, n.d.-u).

### 4.2.2 The Wind Resource

When adding the wind resource to the HOMER Pro model, the configuration of wind turbine parameters and height variations is necessary to simulate the models accurately. According to HOMER Energy (n.d.-n), the software automatically sets the data parameters for the selected location's region based on the imported data files. In this thesis, the wind inputs are downloaded, edited, scaled, and imported into HOMER Pro from *Renewables.ninja*. The wind energy output is calculated using baseline data from the imported file's hourly time steps, which represents the average wind speed (in meters per second) for each month of the year. The average monthly wind speed is shown in the graph below as yellow rectangles (see Fig. 8).

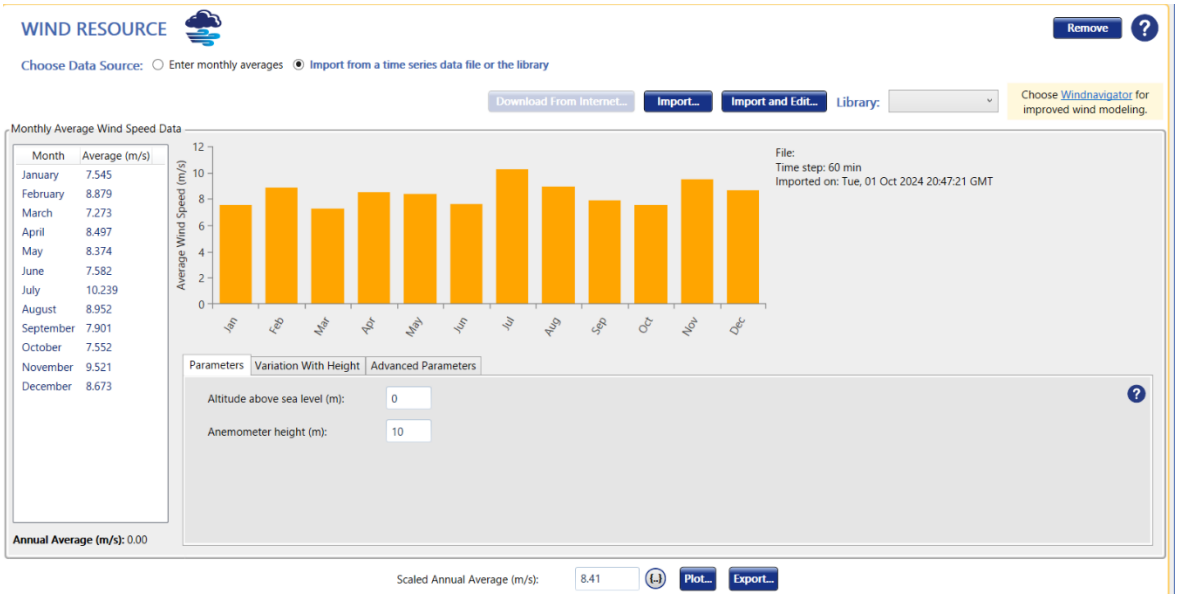


**Figure 8.** Wind Resource for Tasmania.

The turbine parameters include the altitude of the turbine above sea level and the anemometer height, which refers to the distance from the ground level to the point where wind speed data is measured (HOMER Energy, n.d.-ab). These altitude parameters affect the generated wind energy, as wind speed varies with altitude (HOMER Energy, n.d.-ae, n.d.-ac). At ground level, wind speeds tend to be slower due to obstacles such as vegetation and buildings, compared to the wind speeds at the hub height of the turbines (HOMER Energy, n.d.-ac). This variation in wind speeds with height is known as wind shear. To account for this, HOMER Pro allows the selection of a wind speed profile from the *Variation with Height* tab. Using the selected profile, HOMER Pro automatically calculates the wind speed at the turbine's hub height (HOMER Energy, n.d.-ac).

There are two primary mathematical models for calculating wind shear: the *Logarithmic Profile* and the *Power Law Profile*. Depending on the chosen parameters for calculating wind speed ratios, the appropriate mathematical model is selected for the simulation (HOMER Energy, n.d.-ac).

## 4.3 Major Components

The selection components are determined by the scope of the microgrid (see Fig. 3). The components incorporated into the model include Wind Turbine, Photovoltaic Panel (PV panel), Battery, Hydrogen Tank, and Electrolyzer. HOMER Pro offers generic configurations for these components. While some parameters remain consistent across all components, such as *Costs*, *Lifetime,* and *Optimization*, these will be explained once and not repeated for each individual component. The cost parameters were sourced from the *2023 Electricity Annual Technology Baseline* (NREL, 2023) (Appendix 2). *Lifetime* parameters were set according to HOMER Pro's component catalogs, with the exception of the battery lifetime. The battery's lifetime is set to 15 years in the models, based on projected technology improvements before 2029 (Smith et al., 2017).

### 4.3.1 Renewable Energy Source Components

With the corresponding resources set into the model, the wind and solar energy components can be added (HOMER Energy, n.d.-b). In HOMER Pro, users can select from a wide variety of turbines and PV panel options or import data from the software's library into the simulation (HOMER Energy, n.d.-ad, n.d.-s). These options vary in terms of costs, performance characteristics, and capacities (HOMER Energy, n.d.-s). Once the turbine or PV panel type is chosen, the component's properties are displayed, and HOMER Pro begins calculating energy production based on the chosen device and the input resource data.

To determine the RES components, HOMER Pro can automatically calculate the component size, quantity, and associated costs for the system. It can also generate cost curve graphs for each component (HOMER Energy, n.d.-d). Automatic sizing can be turned on or off, depending on the simulation's objectives. Additionally, HOMER Pro allows for the creation of maintenance schedules, detailing costs and downtimes for specific tasks, which are crucial for those relying on the microgrid, as downtime can result in substantial daily costs (HOMER Energy, n.d.-ad).

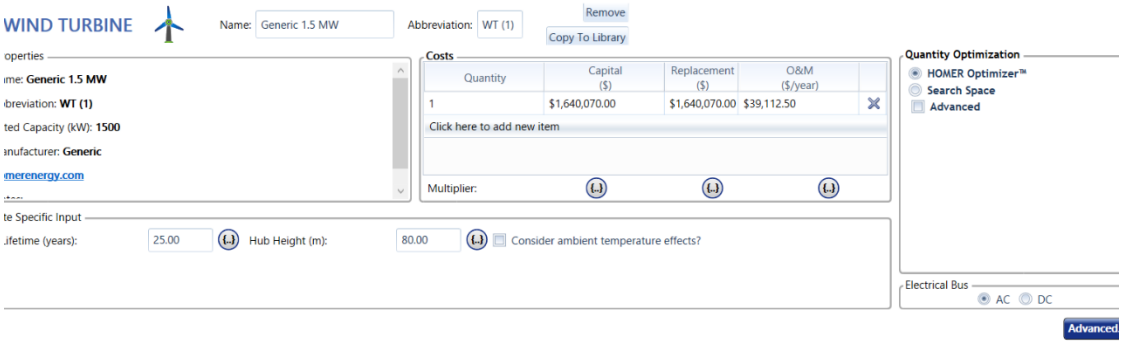


**Figure 9.** Wind Turbine's Default Setup.

Most of the wind turbine parameters and properties are automatically integrated into the simulation from the resource database, load demand inputs, and the selected component's catalog file (HOMER Energy, n.d.-ad). However, some parameters, such as whether the electrical bus operates in AC- or DC-mode, automatic or manual sizing, and site-specific inputs, must be configured manually. Site-specific inputs include the turbine's lifetime, hub height, and the decision to account for ambient temperature effects (see Fig. 10). These parameters must be manually set for the wind turbine system.

The wind turbine can be connected to either the AC or DC bus of the microgrid, depending on the system's design. Automatic sizing can be enabled or disabled based on the simulation's goals. The lifetime parameter, set according to HOMER Pro's component catalog, defines the expected operational duration before the turbine requires replacement (HOMER Energy, n.d.-ad). The Hub Height refers to the distance from the ground to the turbine's hub in meters, and ambient temperature affects air density, which HOMER Pro can adjust for if selected (HOMER Energy, n.d.-ad).

For this thesis, the selected wind turbine type was a 1.5 MW generic wind turbine, with a CAPEX of $1,093.383 and a FOM costs of $26.075 per year (see Fig. 9). The total capacity is determined by the number of turbines in the system and multiplying it with the wind capacities nominal capacity.

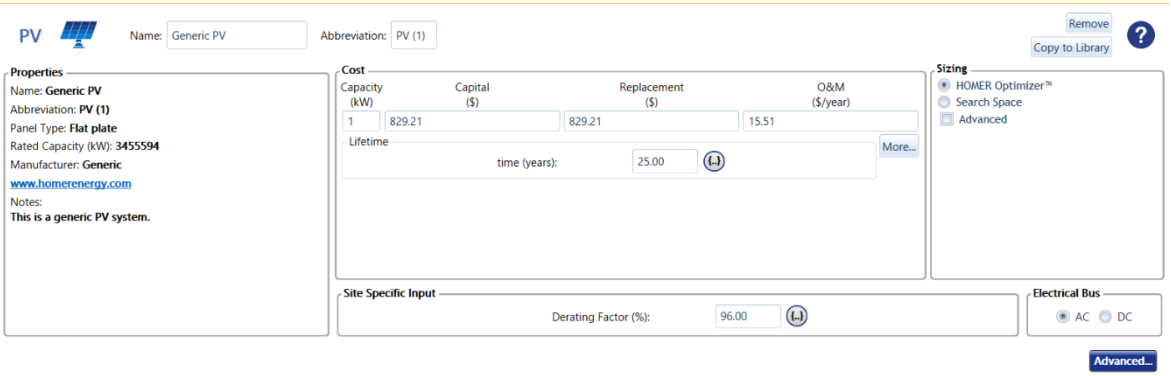


**Figure 10.** Photovoltaic Panel's Default Setup.

Similarly to wind turbines, different PV panels can be chosen from multiple options (Fig. 10). The differences between the options include the cost, performance characteristics, and sizes (HOMER Energy, n.d.-s). HOMER Pro automatically integrates the input data from the catalog file and calculates the solution for the PV panels in the system. As with wind turbines, site-specific inputs such as the *Derating Factor* (%), *Electrical Bus*, and *Sizing* must also be configured. The sizing of the electrical bus follows the same setup as those for wind turbine parameters.

The derating factor accounts for losses accounts for wire losses, dust, and temperature changes, which affect a solar panel's output power. This parameter is set manually, as it is typically too low for a generic panel in 2029; for instance, today's derating factor can be as high as 96% for the *Fronius Primo 8.2-1* PV panel, as per the HOMER Pro catalog.

For this thesis, the selected PV panel is a generic panel with a CAPEX of $529.208 per kW and FOM of $15.518 per kW (Fig. 10). Unlike wind turbines, the capacity of the solar panel is adjusted based on the size of the system, rather than the number of panels.

### 4.3.2 Hydrogen Components

The pages for the hydrogen components, including both the electrolyzer and hydrogen tank, contain cost, performance, site-specific, and other input parameters for the selected component(s) (HOMER Energy, n.d.-d). Modeling hydrogen components in HOMER Pro is relatively straightforward. According to HOMER Energy (n.d.-d), the modeling assumptions include constant efficiency, a minimum load level, and set capacity parameters for both components. Additionally, electrolyzers are assumed to use excess energy unless there is a demand for electricity to produce hydrogen.

In HOMER Pro, there is one generic electrolyzer and one generic hydrogen tank. These components were selected due to the difficulty of obtaining compatible input data. Therefore, technologies such as PEM or AWE electrolyzers and chemical or physical storage for hydrogen are not considered in the simulation models.

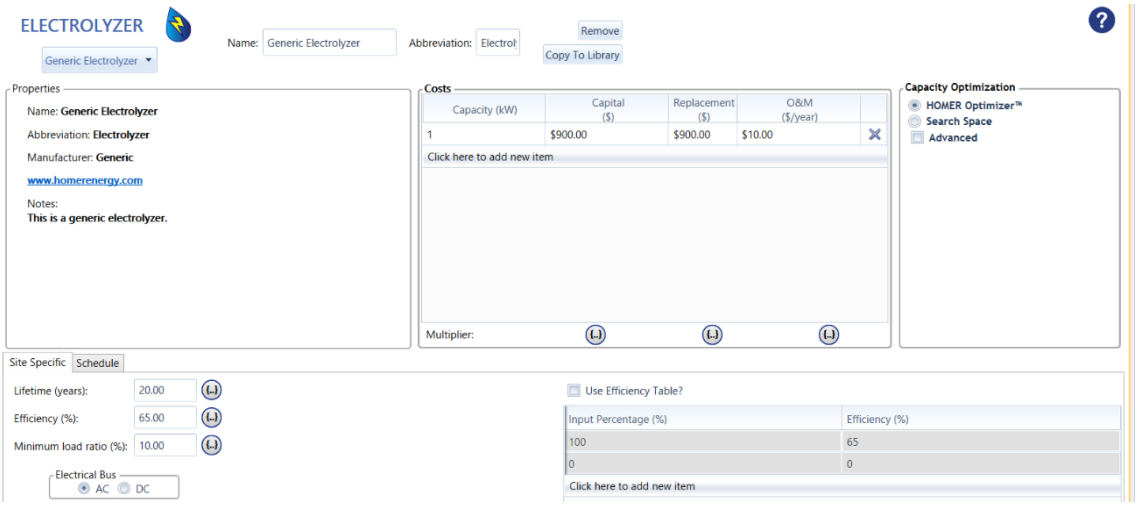


**Figure 11.** Electrolyzer's Default Setup.

The properties of the electrolyzer include several site-specific parameters, such as *Lifetime*, *Efficiency*, *Minimum Load Ratio*, and *Electrical Bus* (HOMER Energy, n.d.-e). The *Lifetime* parameter refers to the number of years the electrolyzer is expected to operate before needing replacement, similar to the lifetime of wind turbines . (HOMER Energy,

n.d.-e). The efficiency parameter (%) represents the ratio of the energy content of the hydrogen produced (based on its higher heating value) to the amount of electricity consumed in the electrolyzing process . (HOMER Energy, n.d.-e). This parameter shows how efficiently the electrolyzer converts electrical energy into hydrogen molecules.

The minimum load ratio indicates the minimum power level at which the electrolyzer can operate at its rated capacity (HOMER Energy, n.d.-d). Operating the electrolyzer below this minimum load ratio can lead to reduced performance, inefficiencies, and potential damage. The electrical bus specifies whether the electrolyzer consumes AC or DC power to produce hydrogen (HOMER Energy, n.d.-d). The choice of AC or DC current affects the electrolyzer's efficiency, costs, and overall system reliability.

The CAPEX for the electrolyzer is $900 per kW, and its FOM is $10 per kW (see Fig. 11). Similar to the PV panel, the electrolyzer's capacity can be adjusted as needed, rather than changing the number of electrolyzer units.

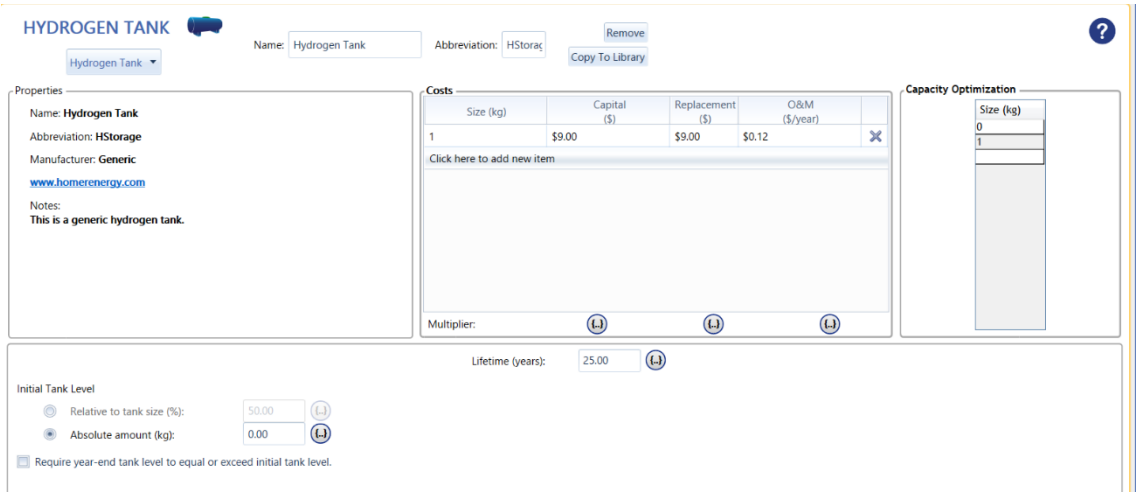


**Figure 12.** Hydrogen Storage's Default Setup.

The hydrogen storage page, includes cost and performance parameters such as the *Initial Tank Level*, *Capacity Optimization*, and *Lifetime Expectancy* (HOMER Energy, n.d.-m). The parameters that differentiate the hydrogen tank from other components are found

under the *Initial Tank Level* section (see Fig. 12). These parameters specify the initial level of the tank at the beginning of the simulation, as a percentage of the tank's size and as an absolute amount in kilograms (HOMER Energy, n.d.-m).

The final parameter for the hydrogen tank is a checkbox that determines whether the year-end tank level must equal or exceed the initial tank level. If this box is checked and the year-end level is lower than the initial level, HOMER Pro considers the system to be infeasible (HOMER Energy, n.d.-m).

The CAPEX for the hydrogen tank is $9 per kg, and its FOM is $0.12 per kg (see Fig. 12). The tank's capacity is measured in the mass of hydrogen it can store.

### 4.3.3 Other Components

This section covers the converter and the BESS components. The capacity determination parameters for these components are consistent with those previously discussed for other components in the system. Both the converter and BESS are selected from HOMER Pro's catalogs, with specific requirements for the BESS to be connected to the DC bus, necessitating the inclusion of a converter.

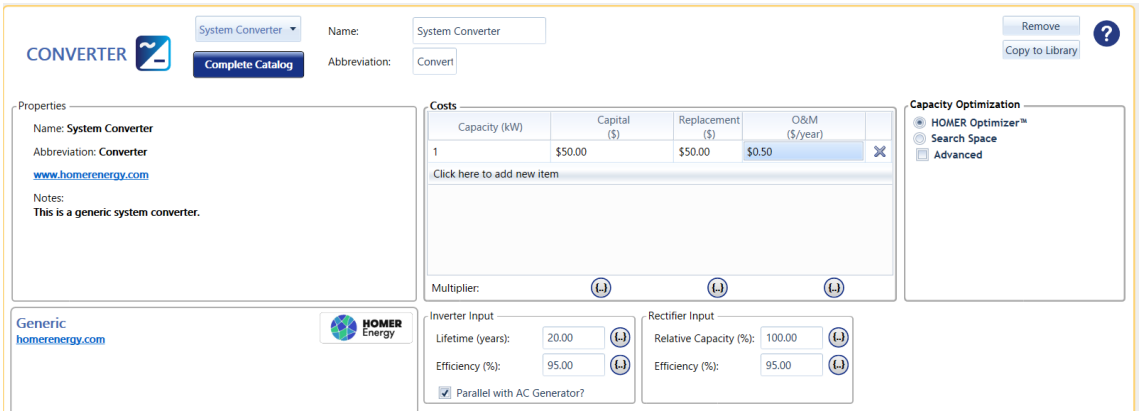


**Figure 13.** Converter's Default Setup.

A microgrid that includes both AC and DC elements requires at least one converter (HOMER Energy, n.d.-c). Similar to other components, some of the converter's parameters depend on the type chosen from the catalog. These parameters include inputs for the inverter and rectifier, costs, and capacity optimization (see Fig. 13). The input parameters for the inverter and rectifier are unique to the converter type. The inverter converts electricity from DC to AC, while the rectifier converts from AC to DC (HOMER Energy, n.d.-c). The inverter and rectifier parameters include lifetime, efficiencies, relative capacities, and whether the converter operates in parallel with an AC generator. In this thesis, generators and their parameters are excluded.

Efficiency of the inverter and rectifier indicates efficiency of conversion of electricity from one to the other (HOMER Energy, n.d.-c). These efficiencies are assumed to be constant in HOMER Pro models and directly affect the efficiency of the converter. The rectifier's relative capacity refers to its rated capacity in relation to the inverter’s capacity (HOMER Energy, n.d.-k). This percentage-based parameter is used as converter components are dedicated to either inverting or rectifying electricity (HOMER Energy, n.d.-k). The relative capacity parameter rates the rectifier’s capacity to the inverter’s capacity (HOMER Energy, n.d.-k). The final parameter is an on/off option that allows users to specify whether the inverter operates in parallel with an AC generator.

The CAPEX for the converter is $50 per kW, and its FOM is $0.5 per kW (see Fig. 13). Similar to the PV panel and electrolyzer, the converter's capacity can be adjusted as needed, rather than changing the number of units.

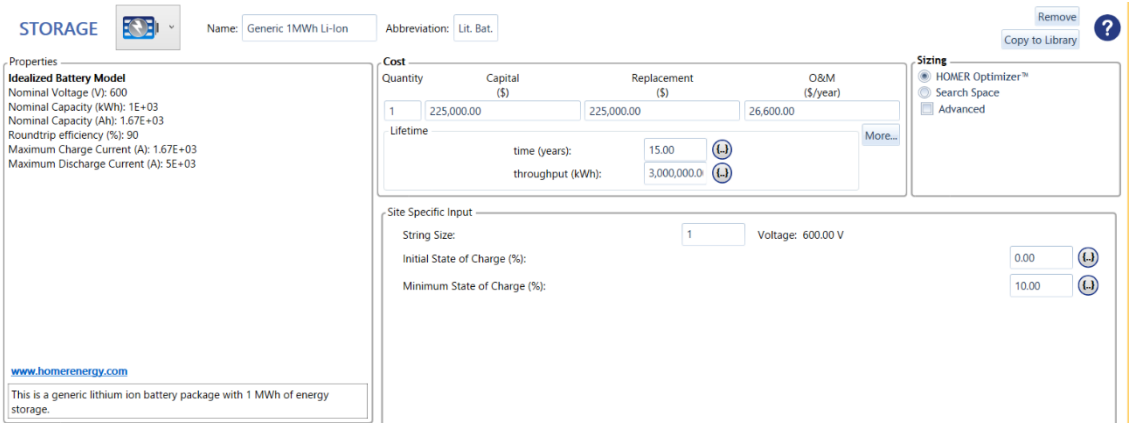


**Figure 14.** Battery's Default Setup.

The electrical storage component chosen for this study was a one megawatt (MW) generic lithium-ion battery. This component features the properties of an *Idealized Battery Model* (HOMER Energy, n.d.-v). Lithium-ion batteries were chosen due to their high efficiency, energy density, performance, and rapid response times. The *Idealized Battery Model* is particularly applicable for modeling high-performance lithium-ion batteries within HOMER Pro (HOMER Energy, n.d.-n). This model includes parameters such as *Nominal Voltage, Capacity, Roundtrip Efficiency,* and *Maximum Charge* and *Discharge Currents.* According to HOMER Energy (n.d.-o), the *Idealized Storage Model* is designed to replicate a storage system that exhibits a flat discharge curve, where the supply voltage remains constant during the discharge cycle. The model enables users to size both energy and power independently by adjusting variables within the software (HOMER Energy, n.d.-v).

The site-specific input parameters for the *Ideal Battery Model* of a lithium-ion battery vary depending on case-by-case scenarios (HOMER Energy, n.d.-n). These storage inputs include *String size*, *Initial State of Charge* (SOC) and *Minimum State of Charge* (MSC). According to HOMER Energy (n.d.-u), the string size refers to a set of storage units, batteries, connected in series. The string size, the number of batteries in series, and the nominal voltage of the batteries are used to calculate the bus voltage. The *Initial State of Charge* indicates the storage bank's charge at the beginning of the simulation, while

the *Minimum State of Charge* defines the lower limit of charge within the model (HOMER Energy, n.d.-v). These SOC parameters are essential in determining the battery's performance and longevity. Proper management of these parameters ensures great performance, extends the operational life of the battery, and prevents premature failure (Monolithic Power Systems, n.d.).

In this thesis, the chosen battery type is the 1.0 MWh generic lithium-ion battery, with a CAPEX of $225,000 and FOM costs of $27,775 annually (see Fig. 14). Similar to the wind turbines, when calculating the battery's capacity in the case studies, the number of batteries determines the total capacity of the system.

# 5 Case Studies

This segment introduces the case studies that are developed later in this study. Table 1 below presents a matrix illustrating the case studies' scenarios. These scenarios were selected to produce outcomes that clearly differentiate the case studies. The models incorporate three different location options and three distinct running-hour profiles. These two variables are combined to create nine case study scenarios, resulting in significantly varied model setups.

**Table 1.** Case Study Matrix.

| | **Good Solar & Wind Resources** (Tasmania) | **Good Solar & Bad Wind Resources** (Bolivia) | **Bad Solar & Good Wind Resources** (Norway) |
|---|---|---|---|
| **24-Hour Method** (Three Shifts) | Case Study 1 | Case Study 4 | Case Study 7 |
| **16-Hour Autonomy Method** (Two Shifts) | Case Study 2 | Case Study 5 | Case Study 8 |
| **8-Hour Autonomy Method** (One Shift) | Case Study 3 | Case Study 6 | Case Study 9 |

The Y-axis of the matrix represents the running-hour profile method of the microgrid. These three different running profile methods are based on the work shift patterns of the APP's workers. During the selected shifts, the demand for both electricity and hydrogen remains constant, stable, and static. However, to meet the plant's daily and yearly demands, the hourly consumption rates of electricity and hydrogen must be adjusted. The plant operates with one, two, or three 8-hour shifts per day, and the methods are categorized as the *24-Hour Method*, *16-Hour Autonomy Method*, or *8-Hour Method*.

The first scenario involves the APP running three shifts, operating continuously throughout the day. This scenario employs the *24-Hour Method*, which calculates the average value of instantaneous loads consuming power over a 24-hour period (Mugo, 2022). As mentioned earlier, studying the effects of varying the running-hour profiles is a key focus of this research. Altering operational hours impacts the load demand profile and, consequently, the calculation method. Instead of maintaining a constant 24-hour demand for hydrogen and electricity, the demand fluctuates during specific periods, prompting the use of the *Autonomy Method*.

According to (Mugo, 2022), the autonomy method refers to the system's ability to operate independently w without external power sources during the defined autonomy period. For the *16-Hour Autonomy Method* and *8-Hour Autonomy Method*, the autonomy period corresponds to two-shift and one-shift load profiles, respectively. These methods meet the same overall load demand as the *24-Hour Method* but within shorter operational periods, leading to significantly higher hourly demand and greater impacts on component capacities in the models.

- In case studies 1, 4, and 7, where the *24-Hour Method* is used, the hourly electricity demand is 30 MW, and hydrogen demand is 5821.9 kg.
- In case studies 2, 5, and 8, using the *16-Hour Autonomy Method*, the hourly electricity demand is 45 MW, and hydrogen demand is 8,732.9 kg.
- In case studies 3, 6, and 9, where the *8-Hour Method* is used, the hourly electricity demand is 90 MW, and hydrogen demand is 17,465.8 kg.

The X-axis of the matrix represents the desired resource characteristics of the selected locations. These characteristics were identified using *the World Wind Atlas* and *World Solar Atlas*. Based on the comparison of solar and wind resources, the following locations were chosen:

- Stanley, Tasmania: Strong solar and wind resources.
- La Paz, Bolivia: Strong solar but poor wind resources.
- Sulsbarmen, Norway: Strong wind resources but poor solar.

Resource profile data files for both solar and wind at these locations were downloaded, processed, and formatted before importing them into HOMER Pro's resource input.

As previously noted, the resource data must be scaled appropriately before being imported into the models. The scaling utilizes the *Trial-and-Test Method*, aligning the model's simulation results with the capacity factor percentages provided by the source website, *Renewables.ninja*. Each location's resource data undergoes this method process, with adjustments applied across all 8,760 timesteps in the data files to achieve realistic modeling. Table 2 (below) collects the scaling multipliers used for the locations.

**Table 2.** Locations Resource's Scaling Multipliers.

| | Tasmania | Bolivia | Norway |
|---|---|---|---|
| Solar's Scaling Multiplier | 0.99 | 0.82 | 0.66 |
| Wind's Scaling Multiplier | 0.78 | 0.84 | 0.79 |

Resource input data files are scaled, they are imported into the case study models. KPIs, which are CAPEX, OPEX, here FOM, LCOE, and LCOH, provide valuable insights for the Decarbonization team regarding the impact of the running hour profiles and locations on the feasibility of future projects.

# 6 The Case Study Models

This section describes the *Trial-and-Test Method* employed in the simulating of the case study simulation models. During this process, several constraints were identified, requiring the implementation of specific simplifications. These simplifications and their implications are discussed in detail in chapter 8, *Discussion*. Additionally, the *Optimizer* was utilized to determine component capacities in the case studies, ensuring results suitable for the objectives of this research.

Before delving into the simulation processes of the case studies, the main steps of these processes are outlined, as all of them follow a similar structure. Detailed processes are presented for Tasmania, Bolivia, and Norway, in that order. For each location, the sequence of methods begins with the *24-Hour Method*, followed by the *16-Hour Autonomy Method*, and concludes with the *8-Hour Autonomy Method*. This sequence is chosen based on the hypothesis that the *24-Hour Method* provides a foundation for models employing autonomy methods.

To begin with, the models are initialized by setting all input parameters, electrical and hydrogen demand, solar and wind resources, component characteristics, and parameters (see Fig. 15).

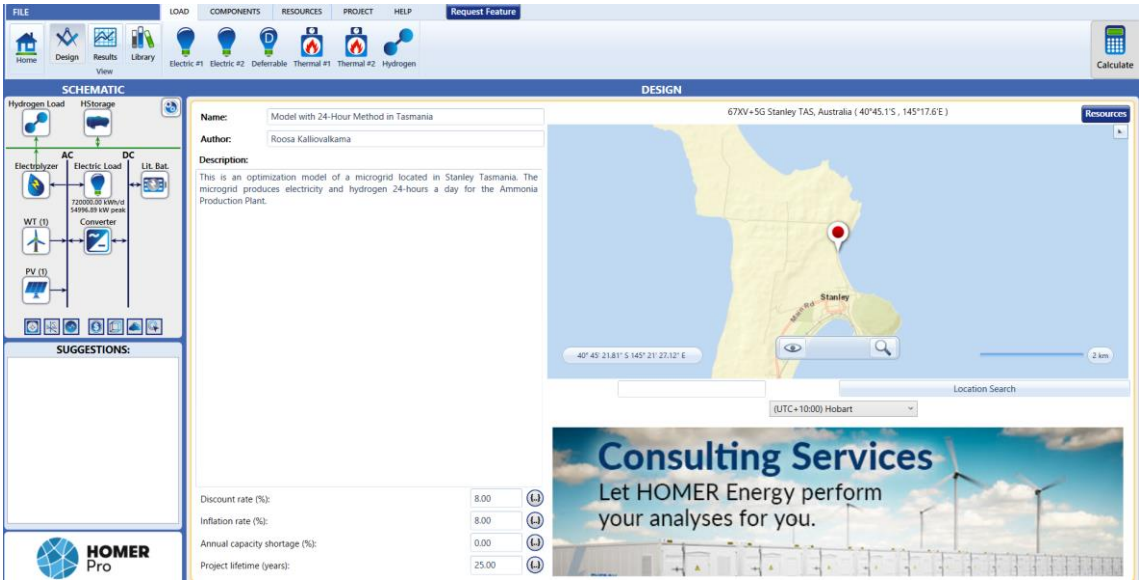


**Figure 15.** Initial Set-Up of the Case Studies.

The *Trial-and-Test* simulation process begins with calculating the capacity of the hydrogen tank. The capacity of which is utilized to minimize excess electricity while keeping the tank size practical. The hydrogen tank, for the *24-Hour Method*, is initially designed to meet daily demand for 10 days, considering maintenance schedules. However, to incorporate a safety margin, the capacity is calculated to cover 14 days of hydrogen demand. This value, determined by multiplying the average daily hydrogen demand (approximately 139,726 kg) by 14 days, yields a maximum tank capacity of 1,956,170 kg. This capacity serves as the initial point for minimizing excess electricity in the simulations results.

In HOMER Pro, the hydrogen tank's capacity was found to impact the amount of excess electricity generated due to the software's coding structure, during the *Trial-and-Test* process. This process then proceeds by gradually reducing the tank's capacity step-by-step, while setting the converter at an overestimated value. The capacities of wind turbines, PV panels, the electrolyzer, and batteries are left for HOMER Pro's *Optimizer* to adjust. Each simulation run checks that the system performance is uncompromised from

the adjustments of the tank's capacity. While the *Trial-and-Test* process is time-consuming, the utilization of this method is essential for achieving a functional base model.

The *Optimizer* is used to determine the hydrogen tank capacity independently, without interference from other components. The converter's capacity is unchanged by HOMER Pro, as the software limits the usage of *Optimizer* for more than four components. Since an overestimated converter capacity has a minimal impact on the hydrogen tank's capacity, it is set to an overestimated value. The hydrogen tank is changed repeatedly until the simulation results yield the minimum level of excess electricity. Once this capacity is identified, it is set in the model.

The next step involves setting the capacities for the wind turbines, PV panels, electrolyzer, and batteries based on the hydrogen tank's capacity as provided by the *Optimizer*. With these values and their costs incorporated into the model, the simulation is run to verify functionality. Ideally, component capacities should remain constant because the *Optimizer* has been used. However, if adjustments are required, the four component capacities are modified incrementally, step-by-step, until the LCOE and LCOH values are minimized with minimal excess electricity.

Once the model meets hydrogen and electricity demands, and component sizes and costs are finalized, the analysis of results can begin. Relationships between component sizes are crucial for the simulation of microgrid models. When the model yields satisfactory results, comparisons are made across factors like resource profiles and their effects on CAPEX and OPEX, aligning with the thesis objectives.

The first hypothesis is that the case studies using the *24-Hour Method* can serve as a baseline for two subsequent case studies conducted in the same location. The second hypothesis is that as the microgrid's operational hours decrease, the capacities of most, if not all, components will also decrease. For example, storage devices, both electrical and hydrogen, are expected to require lower capacities due to the reduced need for

stored energy, as most energy is used immediately. Whether these hypotheses hold will be examined in chapter 7, *Analyzing Results*.

## 6.1 Case Studies of Tasmania

Case Studies 1, 2, and 3 are in Stanley, Tasmania, which has excellent solar and wind resource profiles, making it an ideal starting point for the simulations. As described earlier, the resource data is downloaded, edited, scaled (0.78 for solar and 0.99 for wind), and imported into the model for Case Study 1. These same resources are used for all three running profile scenarios. Case Study 1 is simulated first, to serving as the base setup for the subsequent models.

### 6.1.1 Case Study 1: 24-Hour Method

After importing the solar and wind resource data into HOMER Pro for Stanley, Tasmania, the electrical and hydrogen demands are set to meet the requirements of the APP when using the *24-Hour Method* (30 MW of electricity and 5,822 kg of hydrogen per hour). Other parameters related to the loads are left unchanged in all the case studies.

Next, the components are added to the model (see Fig. 15 above). To ensure the model functions correctly before initiating the *Trial-and-Test* process, the simulation is first run using overestimated component values for all components. As shown in Fig. 16, the overestimated capacity values, which are displayed on the right-hand side in the *Base Case Architecture* (within the red box), yield realistic results, meet the demand, and *Trial-and-Test* process is initiated. According to HOMER Energy (n.d.) the *Winning System Architecture* shows the winning system of the system sizes. This feature is useful, but due to the *Trial-and-Test* process, this result is deemed irrelevant. Once this is done, there should be the only available architecture for the model. Due to this, it will be ignored from further on in this thesis.


**Figure 16.** Tasmania *24-Hour Method Model*'s Overestimated Values.

*Trial-and-Test* process of the hydrogen tank is performed incrementally as it is interdependent for the other components, which can be seen as the other components' capacities, apart from the converter and the hydrogen tank, are set to for the *Optimizer* to determine. The wind turbines, PV panel, electrolyzer, and batteries' capacities are set to the minimum, e.g. one battery and its CAPEX and FOM costs are set according to the minimum capacity values (see Appendix 2), and the *Optimizer* is set on. The *Optimizer* uses these cost values to optimize the component capacities to be as feasible as possible (HOMER Energy, n.d.-r). The converter's capacity is set 500 MW and the hydrogen tank's is set as 1,956,170 kg, and once the simulation is run it shows that the excess electricity is 61.20%, so the *Trial-and-Test* process of the hydrogen tank's capacity is begun.

The hydrogen tank's capacity is reduced incrementally until restatements lead to an increase in excess electricity (Fig. 17). This happens when the hydrogen tank's capacity is 1,934,085 kg and the excess electricity is 28.80%. The next step is to try to determine if the other component capacities could be further decreased. **It is important to note that once the *Optimizer*'s capacities are changed, the *Trial-and-Test* process is deficient due to the synergies between the component capacities.**

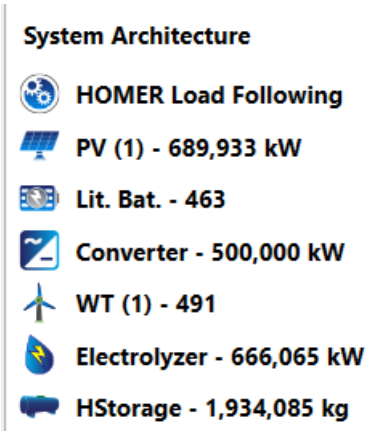


**Figure 17.** Pre-*Trial-and-Test* Process Component Capacities for Case Study 1.

The next step is to find out the relation of the wind turbines and PV panel's capacities, to further decrease the excess electricity. But this unachievable before, the converter and the batteries' capacities, as well as their costs, are set according to Fig. 17 (above). Once converter and batteries' parameters are set accordingly in the model, the relationship between the capacities of PV panels and wind turbines is being adjusted to achieve greater optimization. This is done through *Trial-and-Test* of the number of wind turbines while having the *Optimizer* determines the PV panel's capacity. While the number of wind turbines is increasing, the excess electricity decreases, until the amount of wind turbines is set at 502. This is when the percentage of excess electricity jumps to almost 37%. Once the number of wind turbines decreased back to 501, the percentage decreased to 21.80%. Thus, the number of wind turbines is set to 501 and the PV panels capacity is set to the number it is left on by the *Optimizer*.

Once the PV panel and the wind turbines' capacities and costs are set according to the incrementally modified capacity values, the *Trial-and-Test* process is done for the electrolyzer. Its capacity does decrease slightly. A similar process is done for batteries and converter's capacities that were done for wind turbines and PV panel: the number of batteries is incrementally modified by *Trial-and-Test* process while the converter's capacity is adjusted by the *Optimizer*. The number of batteries is decreased by one, but the

simulation fails to generate results, meaning that the number of batteries was already as minimum as possible. The number of batteries increased back to 463, and the simulation ran again. When this adjustment is done to the capacities, the model produces results. The converter's capacity is set according to the *Optimizer*'s result, costs for the batteries and the converter are updated, and the simulation is run again in order to generate results with the correct costs, like the value of LCOE (Fig. 18 below).

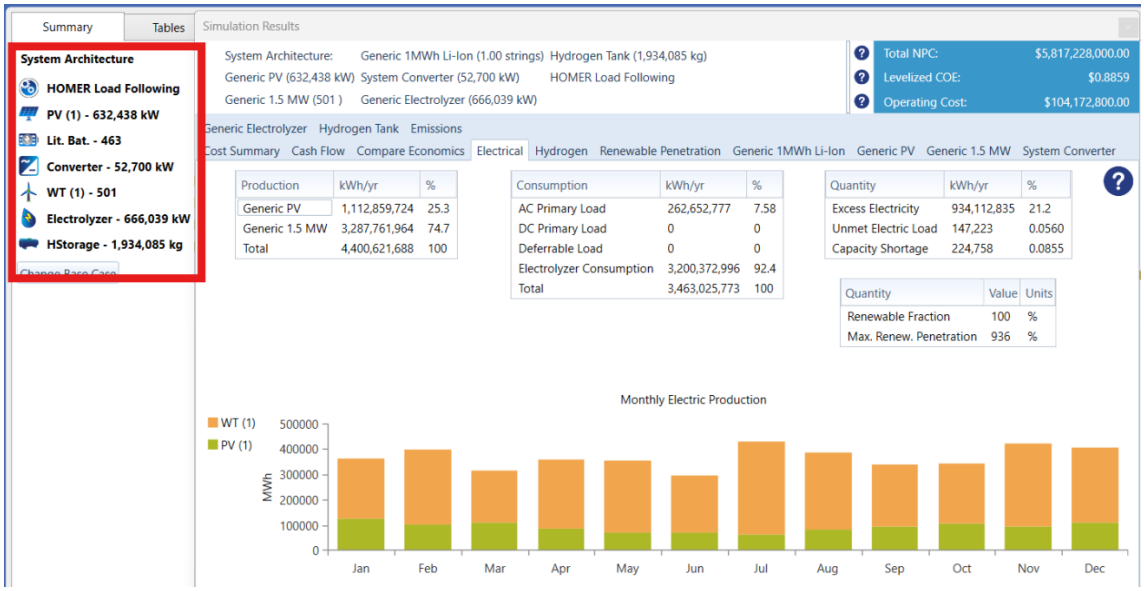


**Figure 18.** Determined Component Capacities for Case Study 1.

From the simulation results pop-up page, illustrated in the figure above, one can view the results for each parameter. The *Simulation Results* section provides access to key outputs, including component capacity factors, emissions, electricity and hydrogen production, among other critical metrics, organized across various tabs. Notably, for components such as the *Hydrogen Tank*, *Generic Wind Turbines* and *Generic PV panels*, replacements are unnecessary due to the project's 20-year lifetime, as shown in Fig. 18 above. From the figure above one can see that the excess electricity decreased to 21.20%.

The results for all nine case studies will be presented, discussed, and analyzed later in this thesis. However, it is important to note that LCOE (in HOMER Pro $/kW) appears unusually high. The LCOE cost should be approximately one-tenth of the current result (Corporate Finance Institute, n.d.). If this trend continues across the other case studies, recalculating the LCOE using alternative software, such as Excel, with the determined parameters from Case Study 1, may be necessary.

### 6.1.2 Case Study 2: 16-Hour Autonomy Method

Since the location remains unchanged, and the hypothesis suggests that component capacities, except for the electrolyzer and converter, should decrease, the simulation model from Case Study 1 serves as the base setup for Case Study 2. The load profiles are adjusted to align with the *16-Hour Autonomy Method*, which defines a demand profile of 45 MW of electricity and 8,733 kg of hydrogen per hour, operating between 5 a.m. and 8 p.m. After incorporating these updated load profiles into the simulation model, performance is verified through simulation.

In this configuration, the capacities of the wind turbines, PV panels, electrolyzer, and batteries are determined by the *Optimizer*, while the converter and hydrogen tank are set to be the overestimated capacities used in Case Study 1. Once these overestimated values are assigned and the model generates realistic results consistent with the parameter settings, the *Trial-and-Test* process begins (Fig. 19).

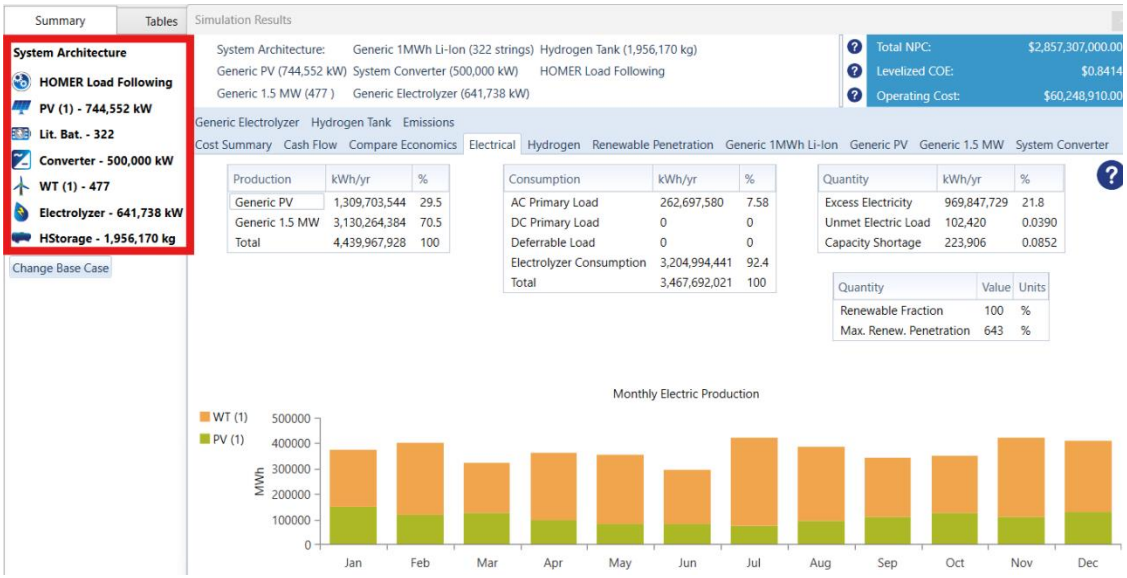


**Figure 19.** Pre-*Trial-and-Test* Process Capacity Values for Case Study 2.

The *Trial-and-Test* process for Case Study 2 follows the same pattern as in the previous model, beginning with the hydrogen tank. It is observed that as the hydrogen tank size is reduced, excess electricity increases. However, due to the overall decrease in LCOE in HOMER Pro and the hypothesis that hydrogen tank's capacity should decrease, this is done through the *Trial-and-Test*. This tank size has a low amount of excess electricity as well as the LCOE cost value in HOMER Pro.

The next steps of the *Trial-and-Test* process are to restate the capacities of the wind turbines, PV panels, electrolyzer, batteries, and converter, each following the same approach as in Case Study 1. The final system architecture, with all determined component capacities, is shown on Fig. 20 (below).

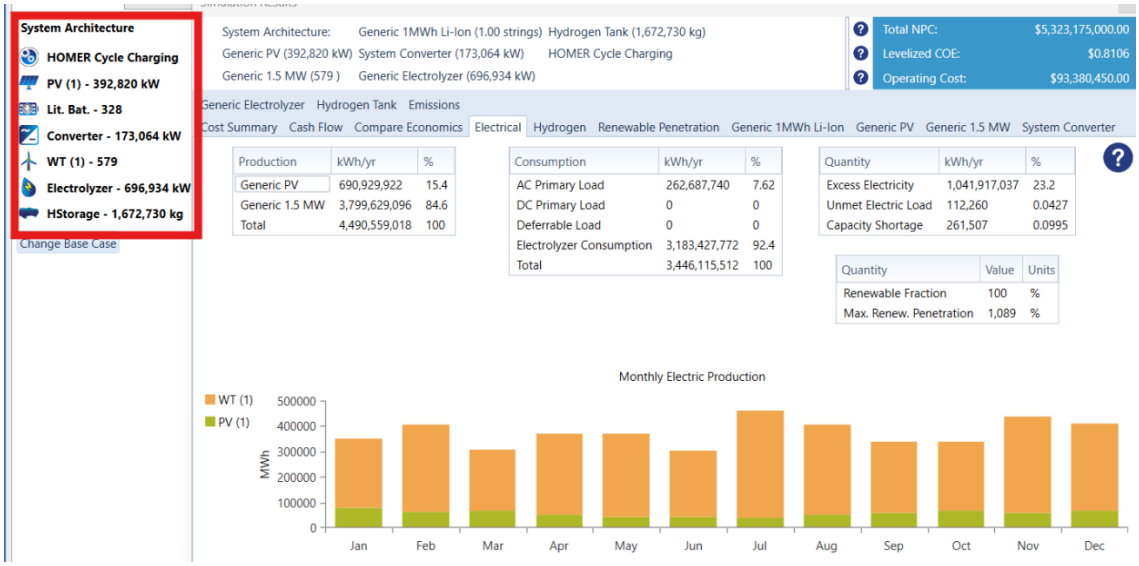


**Figure 20.** Determined Component Capacities for Case Study 2.

Upon completing the *Trial-and-Test* processes for Case Study 2, the converter's component cost is updated according to Appendix 2 and its new capacity. The simulation is rerun with these adjusted costs to verify the results (Fig. 20). The updated results, including the LCOE, the amount of excess electricity, etc., will be used later in the thesis to analyze the simulation results. Similar to the previous case study, however, the LCOE remains unusually high.

### 6.1.3 Case Study 3: 8-Hour Autonomy Method

Since this is the final case study for Stanley, Tasmania, and the hypothesis was confirmed in Case Study 2, it seems reasonable to assume that the *Trial-and-Test* process works for Case Study 3. Therefore, the same process is done for the last case study in Tasmania. As with the previous models, the load profiles must be adjusted to match the operational hours of the method used before the *Trial-and-Test* process begins. For the *8-Hour Autonomy Method*, the demand profile is set to 90 MW of electricity and 17,466 kg of hydrogen per hour, with operations running from 9 a.m. to 4 p.m. Once the updated resource profiles are updated in this model, the performance is ensured by running the

simulation while wind turbines, PV panels, electrolyzer, and batteries' capacities determined by the *Optimizer*, and the converter and the hydrogen tank capacities are set the same overestimated capacity values, as in Case Study 1 and 2 (Fig. 21).

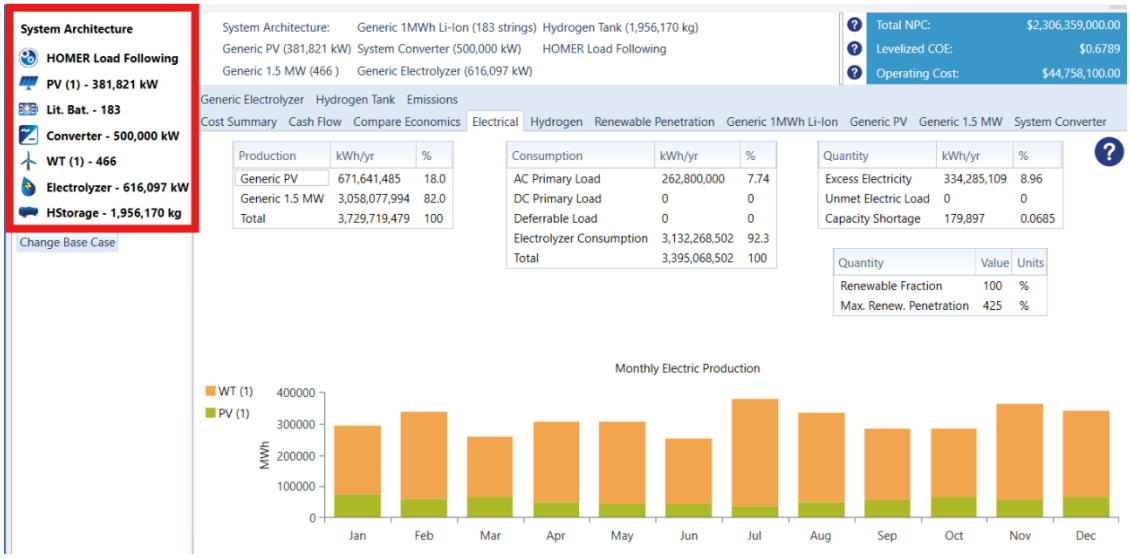


**Figure 21.** Pre-*Trial-and-Test* Process Capacity Values for Case Study 3.

The *Trial-and-Test* process for this model follows the same pattern as in the previous models: component capacities are incrementally reduced, beginning with the hydrogen tank and concluding with the converter, until further adjustments are unfeasible. Similar to Case Study 2, reducing the hydrogen tank size from its initial value leads to a slight increase in excess electricity. However, the LCOE in HOMER Pro decreases significantly. At this capacity, the hydrogen tank achieves both low excess electricity and reduces the LCOE of the system.

Once the hydrogen tank's capacity and its costs are set in the model, the process proceeds in the same pattern as the two previous models and that process is therefore not repeated here. The final system architecture, with determined values for all component capacities and their costs, is shown in Fig. 22. This completes the *Trial-and-Test* process for Case Study 3.

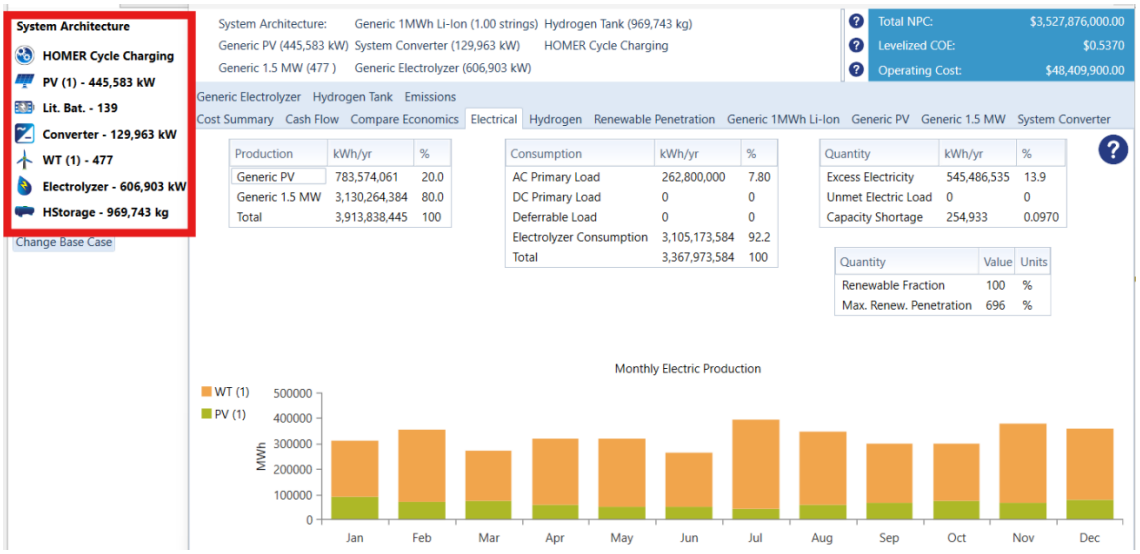


**Figure 22.** Determined Component Capacities for Case Study 3.

The *Trial-and-Test* processes for all three case studies in Tasmania are now complete. The results align with the initial hypothesis: component capacities, except for the electrolyzer and converter, have decreased significantly with the reduced running profiles. In contrast, the capacities of both the electrolyzer and converter have increased substantially. Additionally, it is worth noting that the LCOEs for all three case studies appear unusually high. As this trend persists in the Tasmania case studies, it will be necessary to recalculate both the LCOE and LCOH using the determined parameters later in this thesis.

## 6.2 Case Studies of Bolivia

Case Studies 4, 5, and 6 are based in La Paz, Bolivia, which boasts an excellent solar resource profile but, has a relatively poor wind profile compared to Tasmania. The resource data for La Paz is downloaded, edited, and scaled. Similar to Case Study 1, the data is first applied to Case Study 4, which then serves as the base for the other two models in La Paz. If the *Trial-and-Test* process can be utilized in the Case Study 4, in the same matter as in the previous models, it is utilized in the other two models in Bolivia as well. The load profiles for these three models are the same as those used for the corresponding

methods in the previous cases, and they are set accordingly at the beginning of each model's *Trial-and-Test* process.

### 6.2.1 Case Study 4: 24-Hour Method

As written above, Case Study 4 is created same matter to Case Study 1, and used as a base set up for other two models in Bolivia. Due to both of the demand profiles, components, and most of the other parameters being the same as in Case Study 1, it is used as the base for model of Case Study 4. Parameters, which must be adjusted in the copy of Case Study 1, are the location and the resource data for La Paz's. Once these parameters are changed, the overestimated component capacity values, which are same that were used before, are set in to ensure that the model functions properly with the new location and resource parameters. As shown in Fig. 23 (below), the overestimated capacity values yield realistic results, meeting the demand, and thus the *Trial-and-Test* process is initiated.

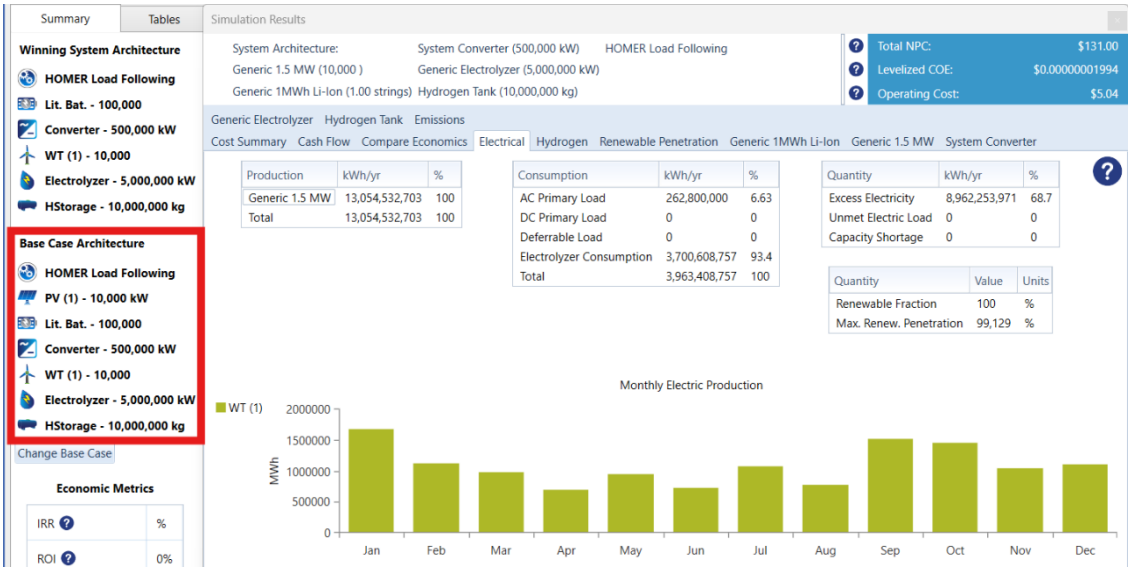


**Figure 23.** Bolivia *24-Hour Method Model*'s Overestimated Values.

The *Trial-and-Test* process for this model follows the same pattern as in the previous three models: the hydrogen tank's capacity is set at 1,956,170 kg, and incrementally decreased until it cannot be reduced to lower the excess electricity. For Case Study 4, this is when the hydrogen tank's capacity is set as 1,945,342 kg and the excess electricity percentage is 66.50%. The next steps of *Trial-and-Test* follow the same pattern as in Case Study 1: wind turbines, PV panel, electrolyzer, batteries, and converter's capacities are incrementally modified in order to reach the desired outcome. The pre-*Trial-and-Test* process values of are illustrated in Fig. 24.

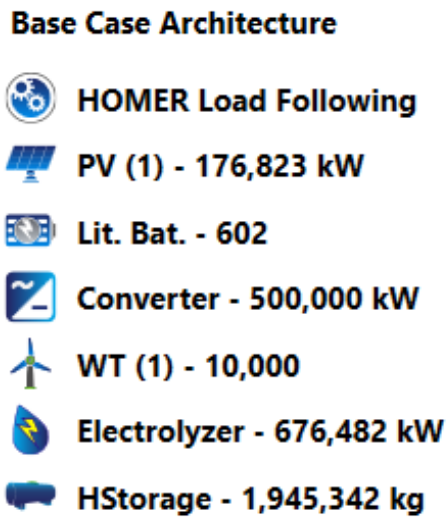


**Figure 24.** Pre-*Trial-and-Test* Process Component Capacities for Case Study 4.

The next step of the *Trial-and-Test* process follows the previous models. When these adjustments are made to the components' capacities, in the order described in Case Study 1, the simulation is run again with the determined cost parameters. This is done in order to attain simulation results with the correct parameters, like the value of LCOE and excess electricity percentage (Fig. 25). This completes the *Trial-and-Test* process of the first model in Bolivia.

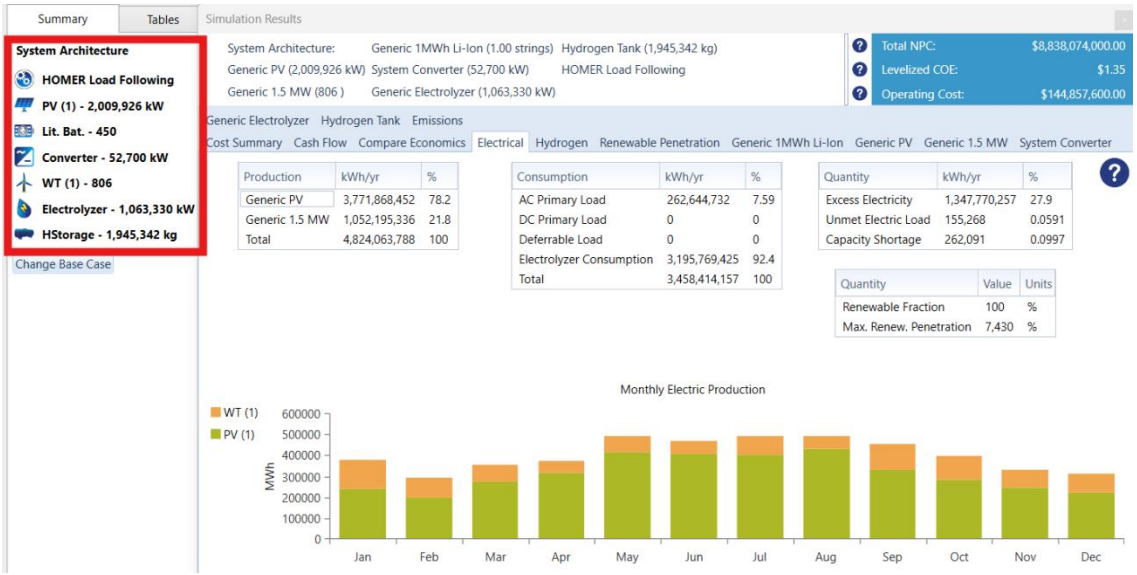


**Figure 25.** Determined Component Capacities for Case Study 4.

Now, the impact of changing the location from Tasmania to Bolivia with the *24-Hour Method* models, can be compared. However, as mentioned earlier, this comparison will be discussed later in the thesis. It is important to note that the LCOE remains unfeasibly high in the initial simulation for Bolivia as well.

### 6.2.2 Case Study 5: 16-Hour Autonomy Method

As observed in the Tasmania case studies, the capacities of most components in Case Studies 4, 5, and 6 are expected to decrease as the operational hours are reduced, except for the electrolyzer and converter, whose capacities are anticipated to increase (electrolyzer) and fluctuate (converter). The adjustments between running profiles and hourly demands of the models in Bolivia, are done in the same way as in the Tasmania case studies. Before beginning the *Trial-and-Test* process a simulation is run using the overestimated values and the *Optimizer*, to ensure the model functions correctly with the adjusted running profile hours. As shown in Fig. 26 (below), the model produces realistic results, allowing the *Trial-and-Test* process to begin.


**Figure 26.** Pre-*Trial-and-Test* Process Capacity Values Case Study 5.

In Case Study 5, the hydrogen tank is incrementally modified down to a capacity of 1,842,300 kg of hydrogen. Once the tank's costs are set accordingly, the *Trial-and-Test* process of the other components begins. Fig. 27 (below) shows the final system architecture, including the determined values for all component capacities, the excess electricity percentage, the LCOE calculated by HOMER Pro, and many other results.

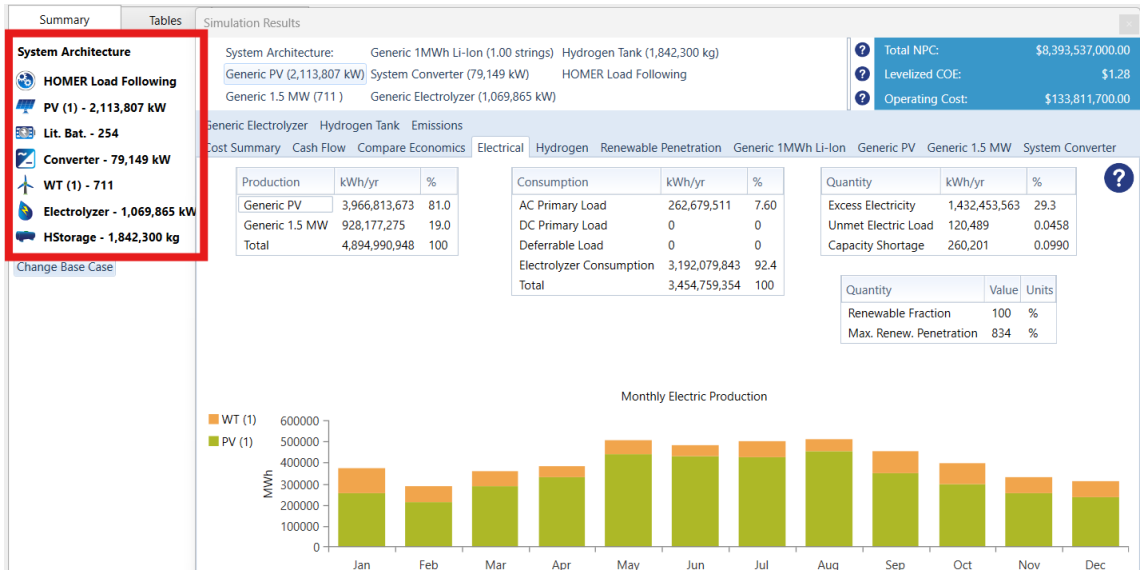


**Figure 27.** Determined Component Capacities for Case Study 5.

Fig. 27 shows the updated results for Case Study 5. The results of this model are analyzed and later on compared between the case studies in Bolivia and the between the case studies utilizing the *16-Hour Autonomy Method*. The trend of LCOE ($/kW) being unfeasibly high continues in the second case study done for Bolivia.

### 6.2.3 Case Study 6: 8-Hour Autonomy Method

Case Study 6 is the final case study for La Paz, Bolivia, and follows the same *Trial-and-Test* processes as in the previous studies done for Bolivia. The only difference between them lies in the running-hour profiles and hourly demands, which are adjusted to match those of Case Study 3. After setting the respective parameters from Case Studies 3 and the overestimated components' capacities, for the hydrogen tank and converter, the model is run before starting the *Trial-and-Test* process to ensure the model functions correctly at this stage, as confirmed in Fig. 28.

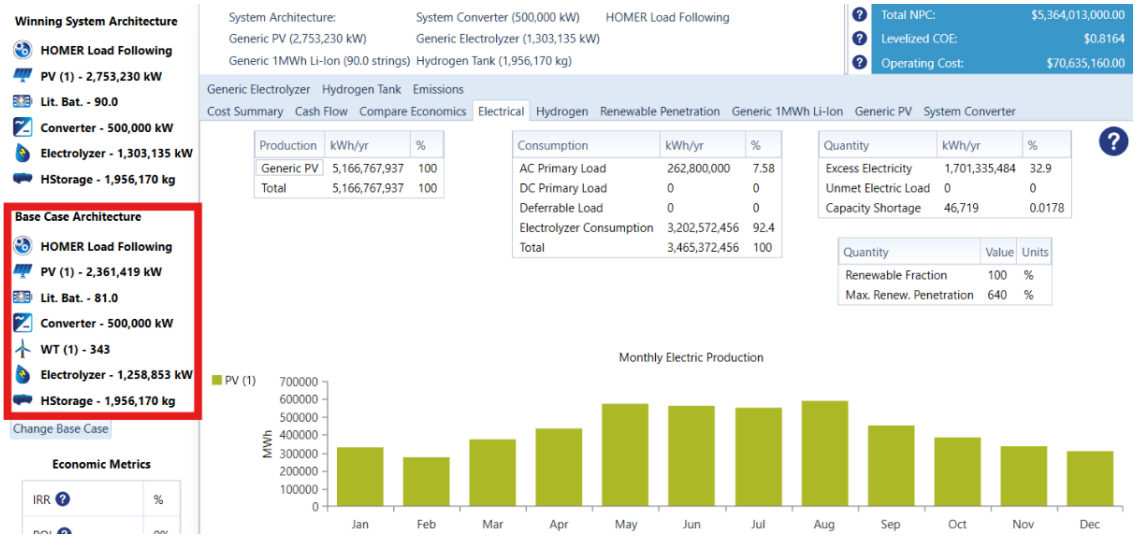


**Figure 28.** Pre-*Trial-and-Test* Process Capacity Values Case Study 6.

The final *Trial-and-Test* process for the models in Bolivia follows the same pattern as the previous ones. In Case Study 6, the hydrogen tank's capacity is incrementally modified down to 893,300 kg, while the excess electricity percentage decreases to 29.30%. The

*Trial-and-Test* rounds of the other component's capacities continue in the same matter as in the previous five case study models, until the limits are reached (Fig. 29).

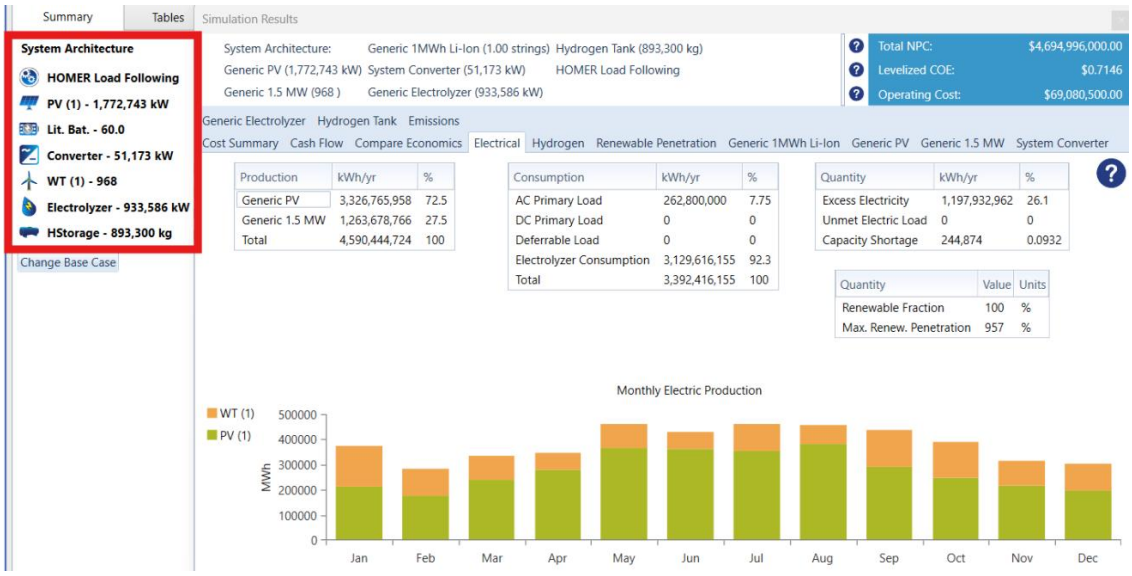


**Figure 29.** Determined Component Capacities for Case Study 6.

The three case study models for Bolivia are now completed. The results from Case Study 4, 5, and 6 align with the initial hypothesis done for Tasmania as well as the results received from them. Also, interestingly the high LCOE price is ongoing within the results from Bolivia, which make it important to see if the trend continues in case studies located in Norway.

## 6.3 Case Studies of Norway

The final three case studies (7, 8, and 9) are situated in Sulsbarmen, Norway, where solar resources are limited, but wind resources are abundant. The resource data for Sulsbarmen was downloaded, adjusted, and scaled at 0.66 for solar and 0.79 for wind. As in the other two locations, this data is initially applied to the model using the *24-Hour Method*. Case Study 7 serves as a base for the remaining two models, which are also based in Norway. The load profiles and corresponding operational hours for these three models

remain consistent with previous cases and are set accordingly at the beginning of each model's *Trial-and-Test* process.

### 6.3.1 Case Study 7: 24-Hour Method

Since the *Trial-and-Test* process from Case Study 1 proved effective for Case Study 4, it is assumed that it can be similarly applied to Case Study 7 with minor parameter adjustments. Specifically, the parameters modified in the copy of Case Study 1 are the location and resource data for Sulsbarmen. Following these adjustments, the previously used overestimated component capacities and the *Optimizer* are applied to confirm that the model functions correctly in Norway with the updated resource parameters. As shown in Fig. 30, with these modifications, the model meets the demand, allowing the restating of the hydrogen tank's capacity to begin.

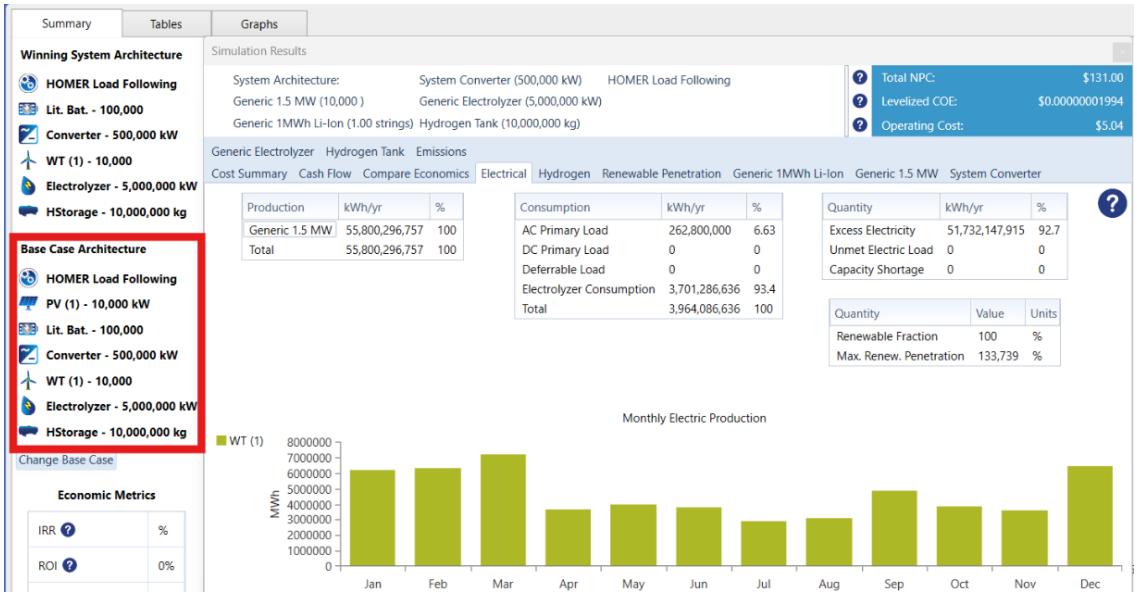


**Figure 30.** Norway *24-Hour Method Model*'s Overestimated Values.

The *Trial-and-Test* process for this model follows the same steps as previous models using the *24-Hour Method*: the hydrogen tank's capacity is initially set to 1,956,170 kg and is incrementally reduced until both the LCOE and excess electricity percentages are at an

acceptable relation, with the converter's capacity set at 500 MW and other components determined by the *Optimizer*. In this case, this configuration is achieved when the hydrogen tank's capacity is reduced by six kilograms, resulting in an excess electricity percentage of 48.60%. Once the hydrogen tank's capacity is set to 1,956,163 kg and updated with corresponding costs, the simulation is rerun (Fig. 31).

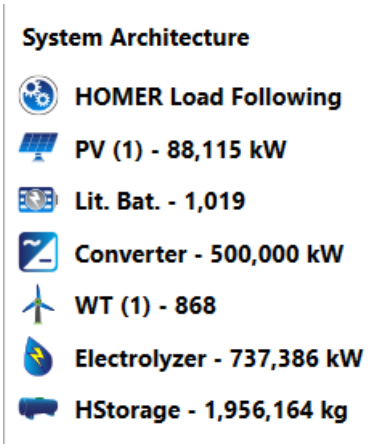


**Figure 31.** Pre-*Trial-and-Test* Process Component Capacities for Case Study 7.

Subsequent adjustments follow the same pattern as before, restating the capacities of the wind turbines, PV panels, electrolyzer, batteries, and converter to reach the limits of the model. Norway's models repeat the process in the previous models. Fig. 32 (below) illustrates the final system architecture, with all determined component capacities included.


**Figure 32.** Determined Component Capacities for Case Study 7.

With the *Trial-and-Test* process complete for Case Study 7, comparisons can now be made between the models in drastically different locations using the *24-Hour Method*. For example, in Case Study 7, the PV panel capacity is reduced to 0 kW, a result that was not identified in any other components during the simulations. A more detailed analysis will be provided later in this thesis, as the remaining two models in Norway need to be incrementally modified, to the same levels of the previous models, for a comprehensive comparison across all case studies. Notably, LCOE values remain prohibitively high across all models using the *24-Hour Method*, suggesting that this trend will likely persist across all nine case studies.

### 6.3.2 Case Study 8: 16-Hour Autonomy Method

Case Study 8 follows the same approach as the previous models and, like Case Studies 2 and 5, utilizes the *16-Hour Autonomy Method*. The previous model from Norway serves as the base setup for Case Study 8, with adjustments made to meet the specific operational hours and hourly demands of the *16-Hour Autonomy Method*. Once updated, the *Optimizer* and overestimated capacity values are applied, as before. The simulation is

then run to ensure that the model's performance remains unaffected by these adjustments. As shown in Fig. 33, the model produces realistic results at this stage, enabling the start of the *Trial-and-Test* process.

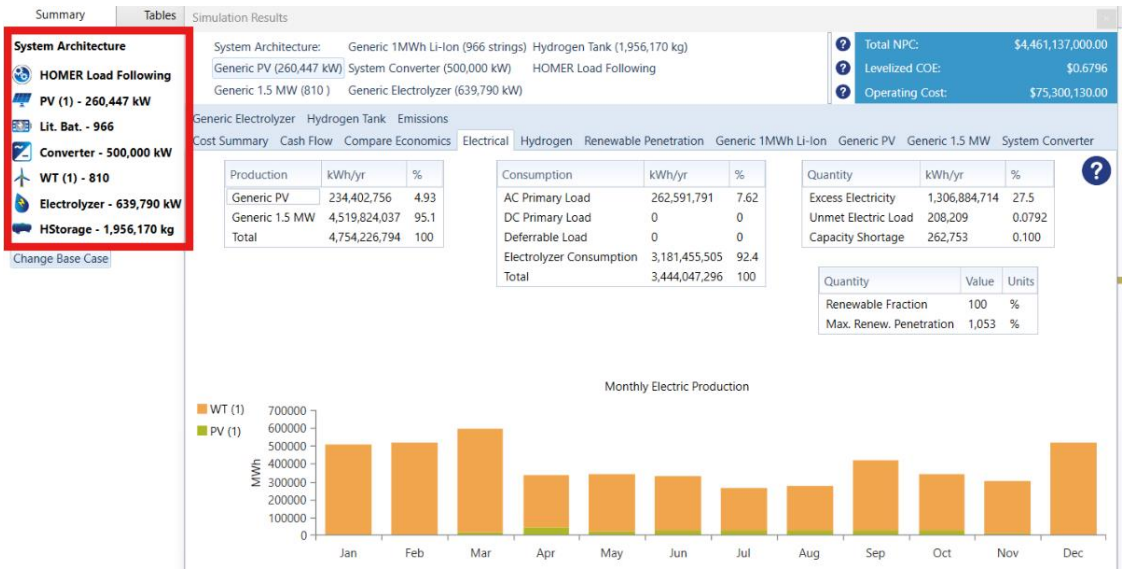


**Figure 33.** Pre-*Trial-and-Test* Process Capacity Values from Case Study 8.

The *Trial-and-Test* process for Case Study 8 mirrors that of previous models and is not repeated here in detail. As with Case Study 7, adjustment of hydrogen tank's capacity is done even though it requires a slight increase in excess electricity to lower the LCOE. The hydrogen tank's capacity is incrementally modified until it is set at 1,250,380 kg, where the excess electricity is 37.30% of the produced electricity. The *Trial-and-Test* process continues similarly to previous case studies. Fig. 34 (below) illustrates the results after the adjustments and that through it, the excess electricity percentage decreased by over 10%. Despite achieving the results wanted, the LCOE remains prohibitively high.

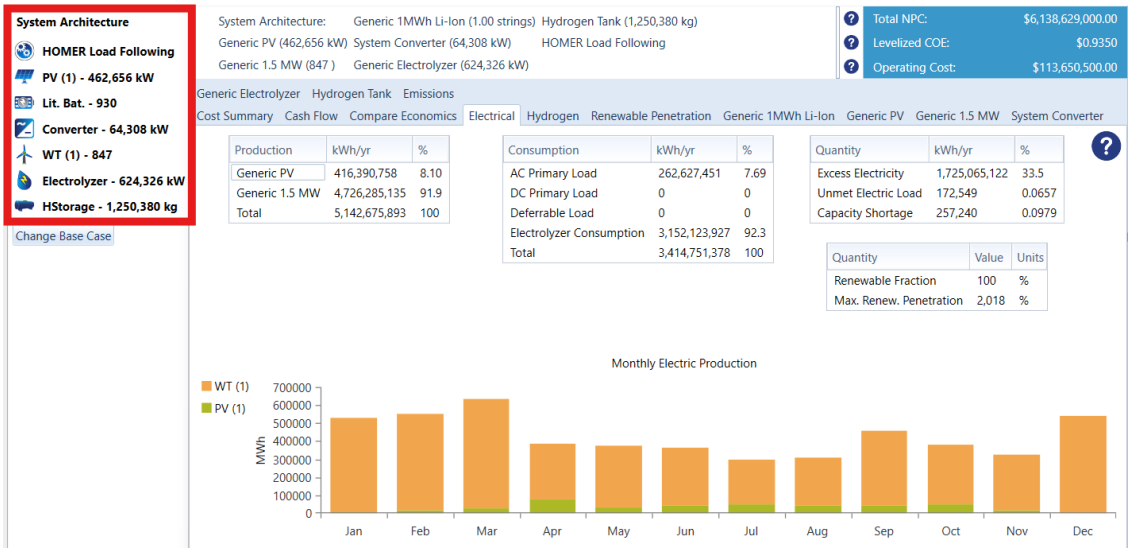


**Figure 34.** Determined Component Capacities for Case Study 8.

### 6.3.3 Case Study 9: 8-Hour Autonomy Method

Case Study 9, the final study in this thesis, is based in Norway and uses the same operational hours and demand profiles as the other two models applying the *8-Hour Autonomy Method*. This approach aligns with the methodology used in the previous eight models, as the *Trial-and-Test* process has proven effective for achieving some level of the determined results. Once all input parameters are configured, a preliminary simulation is run to verify model performance before beginning the *Trial-and-Test* process. After confirming the initial setup (see Fig. 35), the *Trial-and-Test* proceeds in the same manner as in prior models.


**Figure 35.** Pre-*Trial-and-Test* Process Capacity Values Case Study 9.

The final *Trial-and-Test* process follows the same pattern as all previous models. This process continues as before, until all components reach their limits, which are illustrated in Fig. 36 (below).

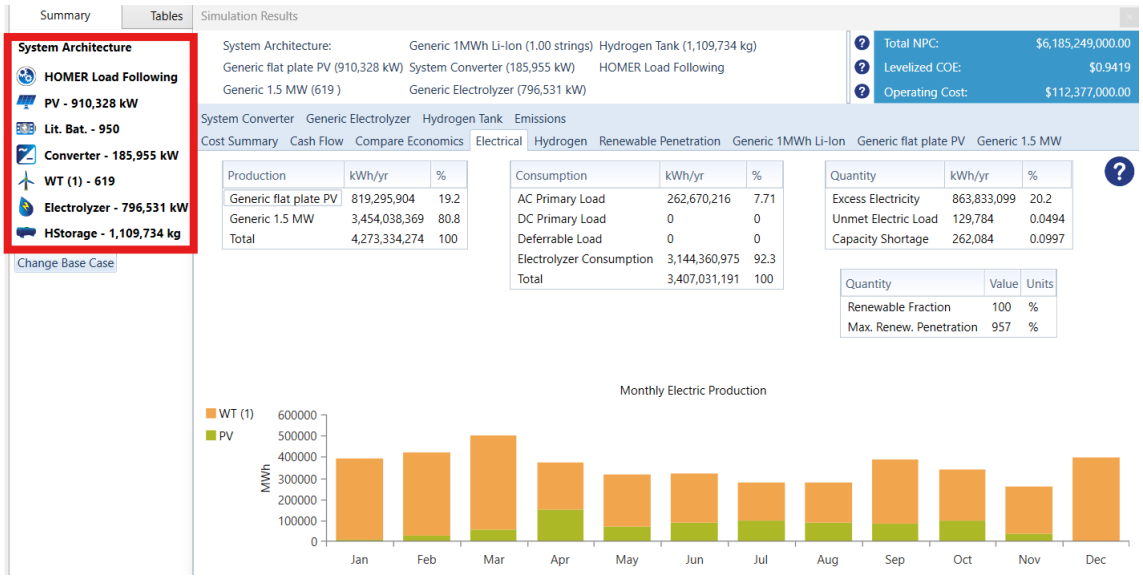


**Figure 36.** Determined Component Capacities for Case Study 9.

The results of the last model confirm that this trend of high LCOE persists throughout all case study model simulations. This may be due to a parameter being set incorrectly or HOMER Pro's incapability to calculate LCOE with the set parameters. Whatever the reason for that is, it is clear that the LCOE and LCOH values must be calculated. The calculation process, previously explained, is completed and analyzed alongside other results in the next chapter.

# 7 Analyzing Results

This chapter presents, discusses, compares, and analyzes the key results of the case studies, which are central to understanding the objectives and scope of this research. These results, including levelized cost values and component capacities, are introduced here, with further comparative analysis provided later in the chapter.

As previously mentioned, the results of the case studies remain deficient. During the *Trial-and-Test* modeling process, several constraints were identified, both within the software and in the resources available for this study. Consequently, the models are unlikely to represent optimized solutions. Nonetheless, this analysis is based on the available outcomes, as preliminary **results remain scientifically valid**. Additionally, exclusions, constraints, simplifications, and recommendations for future studies are discussed in detail in chapter 8, *Discussion*.

However, before proceeding with a detailed analysis, the LCOE and LCOH values are recalculated to address a consistent trend of unfeasibly high LCOE across all case study simulations. As noted earlier, this issue may stem from a misconfigured parameter or a limitation within HOMER Pro when calculating LCOE and LCOH under the specified parameters. Regardless of the root cause, recalculating these costs is critical to ensuring the accuracy of the analysis. A thorough understanding of the cost implications is necessary before advancing to more in-depth evaluation and comparative analysis of the case studies.

## 7.1 Recalculation of the LCOE & LCOH Values

The issue of unfeasibly high LCOE values in HOMER Pro's results across all nine case studies is a critical factor that requires consideration when analyzing the outcomes. HOMER Energy (n.d.-p) defines LCOE as “the average cost per kWh of useful electrical energy produced by the system” (HOMER Energy, n.d.-p). The software calculates LCOE by

dividing the annualized cost of electricity production by the total electricity served within the microgrid (HOMER Energy, n.d.-p). However, HOMER Pro fails to compute LCOH values for case studies. Consequently, these values are calculated utilizing Microsoft Excel, as explained before in this thesis, and analyzed in this section.

High LCOE values calculated by HOMER Pro, manually recalculating them using the determined capacity values is essential to provide a more accurate and realistic assessment of the models' cost-effectiveness. The recalculation process for both LCOE ($/MWh) and LCOH (expressed as $/MWh and $/kg) follows a consistent methodology across all nine case studies, differing only in the specific parameters applied to each. For clarity, this section details the recalculation process using Case Study 1 as an example, as the same method is applied uniformly across the remaining case studies. Notably, hydrogen storage costs are excluded from these calculations due to their inconsequential impact on overall costs.

The recalculation process adheres to the method described earlier in this thesis. Once recalculated with Excel, the updated LCOH ($/kg), LCOE ($/MWh), and LCOH ($/MWh) values for each case study are included in Table 3, alongside the percentage of excess electricity as derived from HOMER Pro's results. The inclusion of excess electricity percentages facilitates a more comprehensive analysis of the results.

**Table 3.** The Final LCOE, LCOH, and the Excess Electricity Values of the Case Studies.

| | LCOE ($/MWh) | LCOH ($/MWh) | LCOH ($/kg) | EXCESS ELECTRICITY (%) |
|---|---|---|---|---|
| **Case Study 1** | $41.11 | $95.89 | $2.88 | 21.20% |
| **Case Study 2** | $37.19 | $91.55 | $2.75 | 23.20% |
| **Case Study 3** | $36.22 | $112.05 | $3.36 | 13.90% |
| **Case Study 4** | $75.62 | $168.40 | $5.05 | 28.10% |
| **Case Study 5** | $70.64 | $161.04 | $4.83 | 29.30% |
| **Case Study 6** | $76.91 | $164.95 | $4.95 | 26.10% |
| **Case Study 7** | $44.97 | $102.80 | $3.08 | 34.90% |
| **Case Study 8** | $49.93 | $107.81 | $3.23 | 33.50% |
| **Case Study 9** | $59.97 | $131.85 | $3.96 | 20.20% |

These recalculated values provide a more accurate and realistic assessment of the cost-effectiveness of the microgrid models. By enabling direct comparisons across the nine case studies, the KPIs, recalculated LCOE, LCOH, and excess electricity, offer insights into the feasibility of each microgrid models' configuration. These results are pivotal in assessing the overall viability and implementation potential of the models, serving as a foundation for the analysis and discussions throughout this study.

## 7.2 Key Results and Hypotheses

The KPIs results are central to the objectives of this thesis as well as the determined component capacities, along with their relationships across different locations and methods. These KPIs results are summarized below, with a more in-depth analysis provided in the next chapter. Tables 4, 5, and 6 (below) present the determined component capacities from the case studies, organized by location. **It is important to note that the *Trial-and-Test* process results remain deficient due to constraints identified during the simulations models.** Hydrogen tank capacity is expressed in terms of the number of days

it can meet the APP's hydrogen demand, as this approach is more intuitive than expressing capacity in kilograms.

Tables 3 through 6 provide the most significant results relevant to the objectives of this thesis, illustrating the influence of locations, resources, and operational hours across the case studies. The *Trial-and-Test* process of adjusting component capacities provided insights into the conditions necessary for developing a microgrid model. This process also highlighted the synergies between microgrid components and the resources required to produce green hydrogen under varying conditions.

As previously noted, the first hypothesis was confirmed: Case Studies 1, 4, and 7, which utilize the *24-Hour Method*, served as the foundation for developing subsequent models in the same locations. However, the second hypothesis could not be fully confirmed. As shown in the tables below, some component capacities, such as those of the batteries and hydrogen tanks, decreased as hypothesized across all three locations with reduced operating hours. Conversely, other components deviate from this pattern. For instance, wind turbine capacities in the Tasmania case studies exhibited a significant increase between Case Studies 1 and 2, rather than the expected decrease. Similar increases were observed in other component capacities across different locations. Numerous factors could explain these discrepancies, and potential reasons for these variations are discussed further in the next chapter, *Further Analysis*.

**Table 4.** Tasmania's Case Studies Determined Values.

| Components | Case Study 1 | Case Study 2 | Case Study 3 |
|---|---|---|---|
| Lithium-Ion Battery | 463 MWh | 328 MWh | 139 MWh |
| Hydrogen Tank | ~14 days | ~12 days | ~7 days |
| Electrolyzer | 668 MW | 699 MW | 958 MW |
| System Converter | 53 MW | 173 MW | 130 MW |
| Wind Turbine | 752 MW | 869 MW | 716 MW |
| Solar Panel | 632 MW | 393 MW | 456 MW |

Table 4 presents the determined component capacities for the Tasmanian case studies, where both wind and solar resources are abundant. Consequently, the results from the first three case studies serve as excellent starting points for comparisons across locations and, subsequently, running hours. As shown in Table 3, the LCOE, LCOH values, and excess electricity percentages in the Tasmanian case studies are the most favorable among the locations examined. Among these, Case Study 3 achieves the most desired outcome, as indicated in Table 3. Additionally, Case Study 2 exhibits the highest excess electricity among the Tasmanian case studies. This outcome stems from the increasing rather than decreasing capacities of certain components, such as wind turbines. Numerous factors could contribute to this trend, but it is most likely influenced by Tasmania's available resources and the balance of RES component capacities, which may be less suited to the *16-Hour Autonomy Method* employed in this case.

**Table 5.** Bolivia's Case Studies Determined Values.

| Component | Case Study 4 | Case Study 5 | Case Study 6 |
|---|---|---|---|
| Lithium-Ion Battery | 450 MWh | 254 MWh | 60 MWh |
| Hydrogen Tank | ~14 days | ~13 days | ~6 days |
| Electrolyzer | 1,063 MW | 1,070 MW | 934 MW |
| System Converter | 53 MW | 79 MW | 51 MW |
| Wind Turbine | 1,209 MW | 1,067 MW | 1,452 MW |
| Solar Panel | 2,010 MW | 2,114 MW | 1,773 MW |

Table 5 presents the determined values for the Bolivian case studies. Bolivia has a relatively abundant solar resource, though its wind resources are limited. As shown in Table 3, the LCOE and LCOH values are the highest among all three Bolivian case studies compared to the other locations. However, the amount of excess electricity in Bolivia does not follow the same pattern observed in Tasmania. Within the Bolivian case studies, the trend in excess electricity aligns with that in Tasmania: it is highest in the case studies using the *16-Hour Autonomy Method* and lowest in those using the *8-Hour Autonomy Method*.

Among the nine case studies, Case Studies 4 and 6 exhibit the least desirable outcomes in terms of LCOE and LCOH values, as indicated in Table 3. Notably, Case Study 6 has the highest LCOE value, while Case Study 4 has the highest LCOH value, making them the least desired according to these metrics.

As noted, while Case Study 6 has the lowest percentage of excess electricity in Bolivia, it also has the highest LCOE value. This outcome is largely due to the model operating only when solar energy is available. During periods of low solar output (e.g. during cloud events), Case Study 6 must rely on wind turbines to meet demand. Given the high CAPEX of wind turbines, this results in the highest LCOE value across all case studies. Similarly, Case Study 4 has the highest LCOH value because it utilizes the *24-Hour Method*, which requires meeting both electricity and hydrogen demands continuously, including during nighttime hours. As wind resources are limited in Bolivia, reliance on wind turbines to meet nighttime demand results in higher model costs.

**Table 6.** Norway's Case Studies Determined Values.

| Component | Case Study 7 | Case Study 8 | Case Study 9 |
|---|---|---|---|
| Lithium-Ion Battery | 1,007 MWh | 930 MWh | 910 MWh |
| Hydrogen Tank | ~14 days | ~10 days | ~8 days |
| Electrolyzer | 675 MW | 624 MW | 796 MW |
| System Converter | 53 MW | 64 MW | 186 MW |
| Wind Turbine | 1,404 MW | 1,271 MW | 929 MW |
| Solar Panel | 0 | 463 MW | 988 MW |

Table 6 presents the final results from the Norwegian case studies, where wind resources are relatively abundant, while solar resources are limited. As shown in Table 3, the excess electricity percentages in the Norwegian case studies are the highest across all three locations. However, as noted earlier, the LCOE and LCOH values in Norway exhibit a different pattern. Like the Bolivian case studies, this divergence from the pattern observed in Tasmania is notable. One exception to the trends observed in both Tasmania and Bolivia is that Case Study 7, which employs the *24-Hour Method*, generates the highest amount of excess electricity among all case studies.

Among the nine case studies, Case Studies 7 and 8 have the least desired outcomes in terms of excess electricity. If this excess electricity is unavailable for use or sale to the larger grid (due to the microgrid operating in islanded mode), or is curtailed in another manner, it may substantially impact the microgrids' stability, affordability, and reliability (Vaziri Rad et al., 2023). With over one-third of the produced electricity classified as excess, these levels are likely to negatively affect the microgrid systems. While all nine case studies show high levels of excess electricity, the levels in Case Studies 7 and 8 are so substantial that, for these microgrids to be feasible, the excess electricity would need to be either stored or sold to the larger grid utilities. However, since microgrids in these case studies are designed to operate in islanded mode, selling excess electricity to the grid is unfeasible.

Another noteworthy finding, unique among the case studies, is observed in Case Study 7: it relies solely on wind power, without utilizing solar resources. As shown in the table above, the solar panel capacity in Case Study 7 is set to zero. This outcome is due to Norway's resource profile and the operational hours specified for this case study. Given that Case Study 7 uses the *24-Hour Method* in a Norwegian setting, solar utilization is unfeasible. This is because wind resources are abundant throughout the day, while solar resources are both limited in availability and constrained by their intermittent nature (see Appendix 6).

## 7.3 Further Analysis

The component capacities across the case studies vary from patterns when analyzed by running hour profiles or by location, except for storage components, which decrease as running hours decrease. As previously noted, various factors contribute to these variations, including the interdependence among components. This section provides further analysis to help draw conclusions from the research. A more in-depth analysis is necessary to reach conclusions and to fully understand how the chosen parameters in each case study impact the irregular relationships among component capacities. In this

segment, particular attention is given to the utilization of the RESs and their profiles, as these have the greatest impact on other components due to inter-component synergies. Appendices 4, 5, and 6 illustrate the resource profiles for the three locations and are referenced in this section.

The Tasmania-based case studies are the most desired in terms of levelized cost values and excess electricity (Table 3), making them the baseline for comparison. In Case Study 1, both wind and solar are fully utilized, with solar available from 7 a.m. to 5 p.m. and wind available for most of the day (Appendix 4). In Case Study 2, wind capacity increases while solar capacity decreases, driven by the increased capacity of the electrolyzer and converter (Table 4). The higher converter capacity allows for more electricity conversion when wind energy is unavailable, while the increased electrolyzer capacity enables more hydrogen production in shorter time steps. Despite the decrease in levelized costs, excess electricity increases by some percentage points (Table 3). Case Study 3 follows the expected trend, with all components showing decreased capacities except for the converter (Table 4). The converter's higher capacity helps compensate for potential weather-induced variability, although not as significant as in Case Study 2, which depends more on wind energy. Solar generation tends to vary less than the wind due to its predictable sunrise and sunset patterns, whereas wind conditions are influenced by multiple, less predictable variables.

The case studies based in Bolivia differ markedly from the previous location due to weaker wind resources. In Bolivia, the trends in RES component capacities vary across different running hours. Specifically, wind capacity decreases from Case Study 4 to Case Study 5, then increases from Case Study 5 to Case Study 6. Conversely, solar capacity increases from Case Study 4 to Case Study 5, then decreases from Case Study 5 to Case Study 6. These shifts result from the different running profiles and varying demand times throughout the day.

In Case Studies 4 and 5, demand is met during the daytime when RESs are available, and storage components are charged as fully as possible. This approach is essential, as both cases rely heavily on energy produced and stored during the day due to limited nighttime resource availability (Appendix 5). Due to this nighttime scarcity, the Bolivia-based microgrids depend more on stored energy than the Tasmania-based case studies. Fig. 37 (below) illustrates the state of charge for lithium-ion batteries in Case Study 4, which follows a similar trend to Case Study 5 and is therefore not separately shown. Compared to Case Study 4, Case Study 5 has higher demand during periods when both solar and wind are available. Given this demand pattern, along with Bolivia's abundant solar capacity, it is more efficient to reduce wind capacity while maintaining solar capacity. In Case Study 6, however, demand occurs only during times when energy sources are available. Because of the relationship between wind and solar capacities and Bolivia's RES capacities, the wind capacity must increase to ensure demand is met, even if solar energy fluctuates during demand hours.

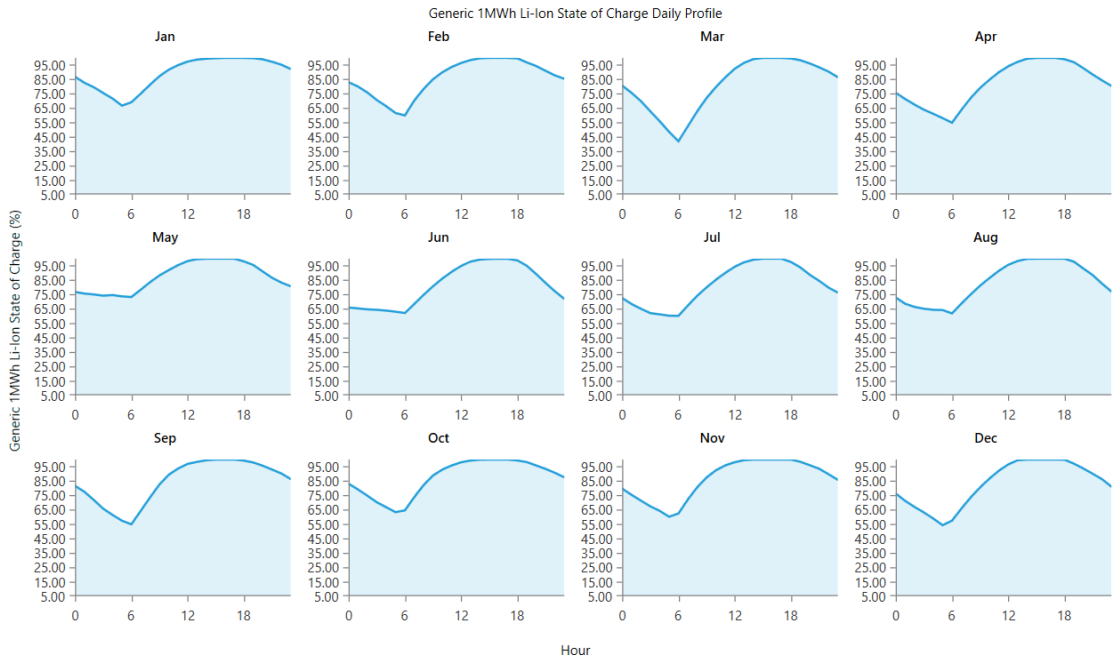


**Figure 37.** Lithium-Ion Batteries State of Charge in Case Study 4.

The RES component capacities in the Norway-based case studies follow a consistent pattern. In Case Study 7, wind component capacity is the highest and solar capacity the lowest, while in Case Study 9, this pattern is reversed (see Table 6). These differences arise from the available RES capacities at each location (Appendix 6) and the running hours of each case. The electrolyzer is the only component in the Norway case studies that deviates from a consistent pattern: its capacity decreases from Case Study 7 to Case Study 8, then increases again from Case Study 8 to Case Study 9. This irregularity may result from multiple factors, likely including variations in capacity factors, as the electrolyzer's capacity change between these later case studies is more pronounced than in other locations.

In Case Study 7, solar energy is excluded due to its low-capacity factor and the 24-hour demand, making its use unfeasible. Instead, a larger capacity of wind energy is more practical than including solar energy. In Case Study 8, however, it becomes feasible to increase solar capacity and reduce wind capacity, as there are more hours when solar energy can be utilized. This trend of increasing solar and decreasing wind component capacity continues in Case Study 9, where even more hours are available for solar energy use.

As shown above, the feasibility of different running profiles varies significantly between locations, though some patterns emerge. Among the profiles, those using the *8-Hour Autonomy Method* show the lowest percentages of excess electricity (Table 3), likely due to the high hourly demand for both electricity and hydrogen, combined with running hours that align with high resource availability (Appendix 4, 5, and 6). However, these cases have among the highest levelized costs, with the exception of the LCOE for Case Study 3 (Table 3). Although Case Studies 3, 6, and 9 had the lowest costs, they are considered the least desired.

Operating a microgrid for eight hours a day is unrealistic in real-world scenarios. A significant amount of renewable energy would be wasted if the grid were unactive when

RESs are available. Shutting down the microgrid at such times would limit its efficiency and overall feasibility by reducing the grid's ability to maximize RES utilization and minimize reliance on stored or backup energy sources. Additionally, intermittent operation would hinder the reliability of the energy supply, which is crucial for cost efficiency and consistent delivery to meet the demand.

Case Studies 2, 5, and 8, which use the *16-Hour Autonomy Method*, tend to have high levels of excess electricity compared to profiles with lower excess electricity percentages (Table 3). This is likely due to the high hourly demand for both electricity and hydrogen, coupled with significant decreases in RES availability during certain hours, depending on the location (Appendix 4, 5, and 6). These fluctuations result in component capacities that are far from the desired relationships. Nevertheless, the levelized costs for Case Studies 2, 5, and 8 are among the lowest in the study (Table 3).

As with the other autonomy-based profiles, discontinuing microgrid operations despite available RESs is likely unrealistic. Case Studies 2, 5, and 8, operating under the *16-Hour Autonomy Method*, are more realistic than those using the *8-Hour Autonomy Method*. However, determining their full feasibility would require additional research, free from the constraints, exclusions, and simplifications discussed later in chapter 8, *Discussion*.

Case Studies 1, 4, and 7 use the *24-Hour Method*, meaning that they operate continuously throughout the day with the lowest hourly demand compared to the autonomy methods. Both the excess electricity and levelized cost values for these models tend to be on the higher end compared to other case studies. The high level of excess electricity is likely because the component capacities are sized to ensure that the microgrid can meet demand even during potential outages of energy sources. However, during periods of high resource availability, excess electricity becomes substantial, impacting the annual excess electricity totals. Higher LCOE and LCOH are likely driven by similar factors.

Operating 24 hours a day may be the most realistic of the running profiles used in this thesis for real-life scenarios, assuming ESs are available. Once the components are installed and the microgrid is running, it seems unfeasible to avoid utilizing the available ESs. Additionally, the *24-Hour Method* offers the benefit of ensuring a stable energy supply, which is crucial in applications where reliability is a priority. However, as previously mentioned, the *24-Hour Method* also has negative impacts on the results, as shown in Table 3. Maintaining a continuous energy supply can also place greater strain on the components, potentially increasing maintenance needs and reducing their lifespan over time. Despite these challenges, the *24-Hour Method*'s ability to deliver consistent power makes it a viable option, particularly for critical applications where reliability outweighs costs and excess generation.

Determining the most feasible simulation model among the nine case study models is possible, though it proved more challenging than initially anticipated due to numerous variables, such as simplifications, comparison baselines, and desired outcomes. If results alone were the primary criteria for identifying the most desired case, Case Studies 1 and 2 would likely offer the most desired outcomes for this research. Both cases feature levelized cost values and excess electricity levels that are among the lowest of the case studies, making them the most feasible solutions overall. The comparatively low values in Case Studies 1 and 2 suggest that the configurations of these models align best with both economic feasibility and efficient utilization of HRESs. These are critical metrics, given the research's focus on the microgrid's ability to meet demand with fluctuating ESs.

Case Studies 1 and 2 rely on consistent availability of RESs in their location. In regions with more variable ESs, alternative configurations may be required for component capacities. This need for adaptability is evident in the results from other locations' case studies. These findings underscore the importance of tailoring microgrid designs to achieve the desired cost and resource efficiency and to meet the specific demands and conditions of each location, as well as the objectives and limitations of the microgrids.

While Case Studies 1 and 2 provide the most favorable baseline for cost and efficiency in this research, further adaptations would be essential if these results were applied in other locations or explored in subsequent research. The location of these case studies, Tasmania, was selected due to its abundant RESs. If the models were to be applied in regions with different characteristics, external factors, such as local weather patterns, storage options, and other environmental parameters, would need to be considered. Future research could build on these findings by investigating the impacts of component adjustments, hybrid operational profiles, or advanced demand fluctuation models. These additional studies could help identify optimized microgrid capacities and performance for diverse, real-world scenarios. A necessary step for future research, however, is to examine the limitations, exclusions, and simplifications that were incorporated into these case study models, which are discussed in the following chapter.

# 8 Discussion

The aim of this research was to analyze green hybrid hydrogen systems across nine case study scenarios and to compare how variations in location and operating profiles affected the performance and KPIs of the microgrid models through techno-economical point of view. The study focused on examining whether component capacities varied with different operating profiles within the same location and assessing the potential of HOMER Pro software for similar studies. Through simulations and analyses of the case studies, answers to these questions were obtained. However, constraints related to both the thesis and the software were also identified during the study.

The research constraints and their effects are elaborated upon here. These fall into two main categories: resource constraints and software constraints. The resource constraints include limited time, familiarity with the software, and funding. Due to these constraints, certain elements were excluded early in the study to simplify and maximize the software's capabilities. Intentional exclusions included selecting generic components and their parameters in HOMER Pro, simulating the case study microgrids solely in islanded mode, and excluding generators and motors. These exclusions were necessary to prevent the thesis from becoming overly broad, which would have further strained available resources.

The second category of constraints relates to the software itself, along with limited expertise in its effective use and understanding of its configurations, such as the computational demands of optimization or the way HOMER Pro applies its optimization algorithm, including the lack of curtailment options. As a result, certain compromises and simplifications were necessary to ensure the models functioned correctly. Examples include using a load-following controller (since HOMER Pro requires a controller), applying identical capacity factors for both wind and solar resources within the same location, and utilizing the *Optimizer*. Once the constraints of this study are explained, these simplifications are discussed in the next chapter.

Among the nine case studies, the most significant constraints of HOMER Pro were its lack of curtailment functionality and the inability of the *Optimizer*'s inability to determine all chosen component capacities simultaneously. The absence of curtailment in the software directly affected the amount of excess electricity and the required component capacities. Combined with the *Optimizer*'s constraints, these issues further restrict the results from achieving the desired results fully. During the *Trial-and-Test* process of each case study, two main constraints of HOMER Pro's *Optimizer* became apparent. However, due to resource constraints, the *Optimizer* was still used.

The first constraint of the *Optimizer* is that users can only determine up to four components per simulation. This constraint is likely due to the optimization algorithm's configuration, which restricts the number of components to reduce computational load. Each additional component expands exponentially increases the number of possible optimization combinations, making the computational demand unfeasible if all components were determined simultaneously. This would make HOMER Pro impractical for its intended purpose, particularly given typical time constraints.

The second constraint of the *Optimizer* is that, among the components used in the case studies, the hydrogen tank was the only one unable to be determined in the same manner as the others. According to HOMER Energy (n.d.), users must manually set the hydrogen tank sizes they want HOMER Pro to consider in the *Capacity Optimization* table, from which HOMER Pro then selects the most desirable size for the simulation. For the other components, the *Optimizer* automatically determines the capacity once the simulation has run.

Several simplifications were applied across the nine case studies, but only the most significant are discussed here, as these were consistent across all cases. As mentioned previously, the components used in the simulations of the microgrid models were generic, with most parameters set to default values from HOMER Pro's catalogs. This decision was made because the objective of this research was to avoid specifying exact

components for each microgrid case study. Additionally, HOMER Pro does not include all types of generic components in its database. For example, it does not distinguish between specific types of electrolyzers or tanks. Therefore, generic components and their standard parameters were used. The decision to exclude specific types of components was made to prevent excessive complexity in the selection process. Another simplification in the case study models involves the renewable energy sources' capacity factors, which were kept consistent across case studies within the same locations.

As mentioned earlier, the profiles for RESs were downloaded, edited, scaled, and imported into the software from *Renewable.ninja*. This website provides data with an hourly timestep, which contributes to more realistic results for case studies using the *24-Hour Method* running profile. However, this level of accuracy is not achieved for the two other running hour profiles used in the study. Although the running profiles were set according to the models, HOMER Pro's inability to incorporate curtailment means that the microgrid models do not actually cease energy production, whether electrical or hydrogen, outside of demand from the APP. This constraint impacts the capacity factors of the RESs in the software, causing HOMER Pro to set identical capacity factors for RESs across case studies within the same location.

Due to resource constraints, manually calculating unique capacity factors for each case study were not feasible. To minimize inaccuracies in the LCOE and LCOH calculations, the annual generation calculations were simplified by using the running hours from the *24-Hour Method* profile instead of those from the *16-Hour* and *8-Hour Autonomy Methods*.

Given these exclusions, resources and software constraints, and other simplifications, further research is recommended to achieve the desired results. Future studies could benefit from increased resources, the use of alternative software or manual calculations, and careful consideration of the exclusions and simplifications made in this study. Furthermore, addressing identified constraints prior to conducting the simulations would significantly enhance the reliability and robustness of the findings. Numerous

opportunities for future research remain, particularly in reevaluating component capacities and exploring their interdependencies, as several questions raised in this thesis remain unresolved. For example, how might the results differ if microgrids were interconnected with a larger grid, allowing for the sale of excess electricity? What changes would arise if specific component types or models were predefined? Moreover, how would an islanded microgrid perform if excess electricity levels were restricted to a normative maximum of 5% (while using HRESs), as suggested by Vaziri Rad et al. (2023).

# 9 Conclusions

This research conducted a techno-economic analysis of green hybrid hydrogen systems across nine case study scenarios using models developed in HOMER Pro software. These hybrid hydrogen systems integrated solar, wind, and storage technologies into microgrid models, aligning with the thesis objective of evaluating techno-economic performance through chosen KPIs: LCOE, LCOH, and the percentage of excess electricity generated. Factors such as operating hours and resource profiles, which influence the capacities of microgrid components, were found to significantly impact the KPIs values. Although the results diverged from initial expectations, they offered valuable insights and guidance for further development, significantly contributing to the field's knowledge base.

The study included a comprehensive review and definition of model parameters for microgrids. Following the establishment of basic model settings, *Trial-and-Test* processes were employed to determine component capacities. However, resource constraints hindered the simulation results of the case study models. During the simulations, it became evident that the available resources were likely insufficient to optimize any of the models. Consequently, certain exclusions and simplifications were necessary to sustain the *Trial-and-Test* process for the case study simulations.

The analysis highlighted the significant influence of location and operating profiles on microgrid performance and costs, two critical factors in the success of the microgrids. This research emphasizes the potential benefits of examining these parameters to enhance the decarbonization in microgrid systems. A thorough understanding and effective utilization of factors such as location, resource availability, and operational hours can drive advancements in the energy sector and optimize the global deployment of renewable energy resources.

## References

Aceves, S., M., Petitpas, G., Espinosa-Loza, F., Matthews, M., J., & Ledesma-Orozco, E. (2013). Safe, long range, inexpensive and rapidly refuelable hydrogen vehicles with cryogenic pressure vessels. *International Journal of Hydrogen Energy*, *38*(5), 2480–2489. https://doi.org/10.1016/j.ijhydene.2012.11.123

Ayers, K. (2019). The potential of proton exchange membrane–based electrolysis technology. *Current Opinion in Electrochemistry*, *18*, 9–15. https://doi.org/10.1016/j.coelec.2019.08.008

Branch, E. (n.d.). *Trial & Error: A Method for Effective Solutions*. IIENSTITU. Retrieved November 17, 2024, from https://www.iienstitu.com/en/blog/trial-error

Corporate Finance Institute. (n.d.). *Levelized Cost of Energy (LCOE)*. Corporate Finance Institute. Retrieved January 24, 2024, from https://corporatefinanceinstitute.com/resources/valuation/levelized-cost-of-energy-lcoe/

David, M., Ocampo-Martínez, C., & Sánchez-Peña, R. (2019). Advances in alkaline water electrolyzers: A review. *Journal of Energy Storage*, *23*, 392–403. https://doi.org/10.1016/j.est.2019.03.001

Directorate General for Energy (European Commission), Trinomics, Badouard, T., Moreira de Oliveira, D., Yearwood, J., Torres, P., & Altman, M. (2020). *Cost of energy (LCOE): Energy costs, taxes and the impact of government interventions on investments : final report*. Publications Office of the European Union. https://data.europa.eu/doi/10.2833/779528

Elexon UK. (2022). *Load Profiles and their use in Electricity Settlement—Elexon Digital BSC*. https://bscdocs.elexon.co.uk/guidance-notes/load-profiles-and-their-use-in-electricity-settlement

European Commission. (n.d.). *European Climate Law—European Commission*. Retrieved November 20, 2024, from https://climate.ec.europa.eu/eu-action/european-climate-law_en

European Commission. (2021, July 14). *The European Green Deal—European Commission*. https://commission.europa.eu/strategy-and-policy/priorities-2019-2024/european-green-deal_en

*European Commission*. (2024). https://www.clean-hydrogen.europa.eu/about-us/key-documents/annual-work-programmes_en

Götz, M. (2016). Renewable Power-to-Gas: A technological and economic review. *Renewable Energy*, *85*, 1371–1390. https://doi.org/10.1016/j.renene.2015.07.066

Gupta, N. (2022). *Trial and Error Method*. eduTinker. https://edutinker.com/glossary/trial-and-error-method/

Haghi, E., Fwoler, M., & Raahemifar, K. (2017). Economic analysis of hydrogen production in context of a microgrid. *2017 IEEE International Conference on Smart Energy Grid Engineering (SEGE)*, 79–84. https://doi.org/10.1109/SEGE.2017.8052780

He, M., Lv, C., Gong, L., Wu, J., Zhu, W., Zhang, Y., Zhang, M., Sun, W., & Sha, L. (2021). The design and optimization of a cryogenic compressed hydrogen refueling process. *International Journal of Hydrogen Energy*, *46*(57), 29391–29399. https://doi.org/10.1016/j.ijhydene.2020.11.061

HOMER Energy. (n.d.-a). *Clearness Index*. Retrieved April 5, 2024, from https://homerenergy.com/products/pro/docs/3.15/clearness_index.html

HOMER Energy. (n.d.-b). *Components Tab*. Retrieved April 8, 2024, from https://homerenergy.com/products/pro/docs/3.15/components_tab.html

HOMER Energy. (n.d.-c). *Converter*. Retrieved April 8, 2024, from https://homerenergy.com/products/pro/docs/3.15/converter.html

HOMER Energy. (n.d.-d). *Electrolyzer*. Retrieved April 8, 2024, from https://homerenergy.com/products/pro/docs/3.15/electrolyzer.html

HOMER Energy. (n.d.-e). *Electrolyzer Efficiency*. Retrieved April 9, 2024, from https://homerenergy.com/products/pro/docs/3.15/electrolyzer_efficiency.html

HOMER Energy. (n.d.-f). *HOMER Pro Hydrogen Module*. Retrieved March 15, 2024, from https://homerenergy.com/products/pro/modules/hydrogen.html

HOMER Energy. (n.d.-g). *HOMER Pro Modules*. Retrieved March 15, 2024, from https://homerenergy.com/products/pro/modules/index.html

HOMER Energy. (n.d.-h). *HOMER Pro Software*. Retrieved March 15, 2024, from https://homerenergy.com/products/pro/index.html

HOMER Energy. (n.d.-i). *HOMER Software Testimonials*. Retrieved March 15, 2024, from https://homerenergy.com/products/pro/testimonials.html

HOMER Energy. (n.d.-j). *Https://homerenergy.my.site.com/supportcenter/s/article/electric-load-data-in-homer2*. Retrieved April 4, 2024, from https://homerenergy.my.site.com/supportcenter/s/article/electric-load-data-in-homer2

HOMER Energy. (n.d.-k). *Https://homerenergy.my.site.com/supportcenter/s/article/modeling-an-inverter-only-or-rectifier-only-with-the-conv*. Retrieved April 10,

2024, from https://homerenergy.my.site.com/supportcenter/s/article/modeling-an-inverter-only-or-rectifier-only-with-the-conv

HOMER Energy. (n.d.-l). *Hydrogen Load*. Retrieved April 4, 2024, from https://homerenergy.com/products/pro/docs/3.15/hydrogen_load.html

HOMER Energy. (n.d.-m). *Hydrogen Tank*. Retrieved April 8, 2024, from https://homerenergy.com/products/pro/docs/3.15/hydrogen_tank.html

HOMER Energy. (n.d.-n). *Idealized Battery*. Retrieved April 26, 2024, from https://homerenergy.com/products/pro/docs/3.15/idealized_battery.html

HOMER Energy. (n.d.-o). *Idealized Model*. Retrieved April 29, 2024, from https://homerenergy.com/products/pro/docs/3.15/idealized_model.html

HOMER Energy. (n.d.-p). *Levelized Cost of Energy*. Retrieved October 14, 2024, from https://homerenergy.com/products/pro/docs/3.15/levelized_cost_of_energy.html

HOMER Energy. (n.d.-q). *Loads Tab*. Retrieved April 4, 2024, from https://homerenergy.com/products/pro/docs/3.15/loads_tab.html

HOMER Energy. (n.d.-r). *Optimization*. Retrieved October 29, 2024, from https://homerenergy.com/products/pro/docs/3.15/optimization.html

HOMER Energy. (n.d.-s). *Photovoltaic Panels (PV)*. Retrieved April 8, 2024, from https://homerenergy.com/products/pro/docs/3.15/photovoltaic_panels_pv.html

HOMER Energy. (n.d.-t). *Resources Tab*. Retrieved April 5, 2024, from https://homerenergy.com/products/pro/docs/3.15/resources_tab.html

HOMER Energy. (n.d.-u). *Solar GHI Resource*. Retrieved April 5, 2024, from https://homerenergy.com/products/pro/docs/3.15/solar_ghi_resource.html

HOMER Energy. (n.d.-v). *Storage*. Retrieved April 8, 2024, from https://homerenergy.com/products/pro/docs/3.15/storage.html

HOMER Energy. (n.d.-w). *Summary With a Base Case and Winning Case*. Retrieved October 8, 2024, from https://homerenergy.com/products/pro/docs/3.15/summary_with_a_base_case_and_winning_case.html

HOMER Energy. (n.d.-x). *Unmet Load*. Retrieved April 4, 2024, from https://homerenergy.com/products/pro/docs/3.15/unmet_load.html

HOMER Energy. (n.d.-y). *Value of Electricity*. Retrieved April 4, 2024, from https://homerenergy.com/products/pro/docs/3.15/value_of_electricity.html

HOMER Energy. (n.d.-z). *Welcome to HOMER*. Retrieved April 4, 2024, from https://homerenergy.com/products/pro/docs/3.15/index.html

HOMER Energy. (n.d.-aa). *Wind Resource Advanced Parameters*. Retrieved April 5, 2024, from https://support.ul-renewables.com/homer-manuals-pro/_wind_resource_advanced_parameters.html

HOMER Energy. (n.d.-ab). *Wind Resource Parameters*. Retrieved April 5, 2024, from https://homerenergy.com/products/pro/docs/3.15/wind_resource_parameters.html

HOMER Energy. (n.d.-ac). *Wind Resource Variation with Height*. Retrieved April 5, 2024, from https://homerenergy.com/products/pro/docs/3.15/wind_resource_variation_with_height.html

HOMER Energy. (n.d.-ad). *Wind Turbine*. Retrieved April 8, 2024, from https://homerenergy.com/products/pro/docs/3.15/wind_turbine.html

HOMER Energy. (n.d.-ae). *Wind Turbine Hub Height*. Retrieved April 5, 2024, from https://homerenergy.com/products/pro/docs/3.15/wind_turbine_hub_height.html

Hu, K., Fang, J., Ai, X., Huang, D., Zhong, Z., Yang, X., & Wang, L. (2022). Comparative study of alkaline water electrolysis, proton exchange membrane water electrolysis and solid oxide electrolysis through multiphysics modeling. *Applied Energy*, *312*, 118788. https://doi.org/10.1016/j.apenergy.2022.118788

Hydrogen Europe. (n.d.). In a nutshell. *Hydrogen Europe*. Retrieved November 14, 2024, from https://hydrogeneurope.eu/in-a-nutshell/

IEA. (n.d.). The Future of Hydrogen. *2019*.

IEA. (2023). *Greenhouse Gas Emissions from Energy Data Explorer—Data tools. A data tool by the International Energy Agency.* IEA. https://www.iea.org/data-and-statistics/data-tools/greenhouse-gas-emissions-from-energy-data-explorer

Jayawardana, A., Agalgaonkar, A. P., Robinson, D. A., & Fiorentini, M. (2019). Optimisation framework for the operation of battery storage within solar-rich microgrids. *IET Smart Grid*, *2*(4), 504–513. https://doi.org/10.1049/iet-stg.2019.0084

Kharel, S., & Shabani, B. (2018). Hydrogen as a Long-Term Large-Scale Energy Storage Solution to Support Renewables. *Energies*, *11*(10), 2825. https://doi.org/10.3390/en11102825

Kojima, H., Nagasawa, K., Todoroki, N., Ito, Y., Matsui, T., & Nakajima, R. (2023). Influence of renewable energy power fluctuations on water electrolysis for green hydrogen

production. *International Journal of Hydrogen Energy*, *48*(12), 4572–4593. https://doi.org/10.1016/j.ijhydene.2022.11.018

Kumar, S. S., & Lim, H. (2022). *An overview of water electrolysis technologies for green hydrogen production—ScienceDirect*. https://www.sciencedirect.com/science/article/pii/S2352484722020625

Lambert, T. (2006). *Micropower System Modeling with Homer*.

Ma, N., Zhao, W., Wang, W., Li, X., & Zhou, H. (2024). Large scale of green hydrogen storage: Opportunities and challenges. *International Journal of Hydrogen Energy*, *50*, 379–396. https://doi.org/10.1016/j.ijhydene.2023.09.021

Madhlopa, A. (2022). *Chapter 2—Solar radiation resource*.

Mancarella, P. (2021). *Green Hydrogen: A Tale From Two Countries - IEEE Smart Grid*. https://smartgrid.ieee.org/bulletins/february-2021/green-hydrogen-a-tale-from-two-countries

Mayyas, A., Wei, M., & Levis, G. (2020). Hydrogen as a long-term, large-scale energy storage solution when coupled with renewable energy sources or grids with dynamic electricity pricing schemes. *International Journal of Hydrogen Energy*, *45*(33), 16311–16325. https://doi.org/10.1016/j.ijhydene.2020.04.163

Microsoft Support. (n.d.). *PMT function—Microsoft Support*. Retrieved October 14, 2024, from https://support.microsoft.com/en-us/office/pmt-function-0214da64-9a63-4996-bc20-214433fa6441

Millet, P., & Grigoriev. (2013). Chapter 2—Water Electrolysis Technologies. In L. M. Gandía, G. Arzamendi, & P. M. Diéguez (Eds.), *Renewable Hydrogen Technologies* (pp. 19–41). Elsevier. https://doi.org/10.1016/B978-0-444-56352-1.00002-7

Mohammad Amin Vaziri Rad, Kasaeian, A., Niu, X., Zhang, K., & Mahian, O. (2023). Excess electricity problem in off-grid hybrid renewable energy systems: A comprehensive review from challenges to prevalent solutions. *Renewable Energy*, *212*, 538–560. https://doi.org/10.1016/j.renene.2023.05.073

Monolithic Power Systems. (n.d.). *The Importance of State of Charge (SOC) and State of Health (SOH) in Battery Management Systems | Article | MPS*. Retrieved April 29, 2024, from https://www.monolithicpower.com/en/the-importance-of-state-of-charge-and-state-of-health-in-battery-management-systems

Moreno-Blanco, J., Petitpas, G., Espinosa-Loza, F., Elizalde-Blancas, F., Martines-Frias, J., & Aceves, S., M. (2019). The storage performance of automotive cryo-compressed hydrogen vessels. *International Journal of Hydrogen Energy*, *44*(31), 16841–16851. https://doi.org/10.1016/j.ijhydene.2019.04.189

Mosca, L., Medrano Jimenez, J. A., Wassie, S. A., Gallucci, F., Palo, E., Colozzi, M., Taraschi, S., & Galdieri, G. (2020). Process design for green hydrogen production. *International Journal of Hydrogen Energy*, *45*(12), 7266–7277. https://doi.org/10.1016/j.ijhydene.2019.08.206

Mugo, S. (2022). *Calculating Load Profile—Technical Articles*. https://eepower.com/technical-articles/calculating-load-profile/

Muyeen, S. M., Islam, S. M., & Blaabjerg, F. (2019). *Variability, Scalability and Stability of Microgrids*. Institution of Engineering & Technology. http://ebookcentral.proquest.com/lib/tritonia-ebooks/detail.action?docID=6026427

Nasser, M., Megahed, T. F., Ookawara, S., & Hassan, H. (2022). A review of water electrolysis–based systems for hydrogen production using hybrid/solar/wind energy

systems. *Environmental Science and Pollution Research*, *29*(58), 86994–87018. https://doi.org/10.1007/s11356-022-23323-y

NREL. (2023). *Technologies | Electricity | 2023 | ATB | NREL*. https://atb.nrel.gov/electricity/2023/technologies

Sadi, M., & Deymi-Dashtebayaz, M. (2019). Hydrogen refueling process from the buffer and the cascade storage banks to HV cylinder. *International Journal of Hydrogen Energy*, *44*(33), 18496–18504. https://doi.org/10.1016/j.ijhydene.2019.05.023

Shahbazbegian, V., Shafie-khah, M., Laaksonen, H., Strbac, G., & Ameli, H. (2023). Resilience-oriented operation of microgrids in the presence of power-to-hydrogen systems. *Applied Energy*, *348*, 121429. https://doi.org/10.1016/j.apenergy.2023.121429

Smith, K., Saxon, A., Keyser, M., Lundstrom, B., Ziwei Cao, & Roc, A. (2017). Life prediction model for grid-connected Li-ion battery energy storage system. *2017 American Control Conference (ACC)*, 4062–4068. https://doi.org/10.23919/ACC.2017.7963578

U.S. Department of Energy. (n.d.). *Hydrogen Production: Electrolysis*. Energy.Gov. Retrieved January 30, 2024, from https://www.energy.gov/eere/fuelcells/hydrogen-production-electrolysis

Vaziri Rad, M. A., Kasaeian, A., Niu, X., Zhang, K., & Mahian, O. (2023). Excess electricity problem in off-grid hybrid renewable energy systems: A comprehensive review from challenges to prevalent solutions. *Renewable Energy*, *212*, 538–560. https://doi.org/10.1016/j.renene.2023.05.073

Wang, M., Wang, Z., Gong, X., & Guo, Z. (2014). The intensification technologies to water electrolysis for hydrogen production – A review. *Renewable and Sustainable Energy Reviews*, *29*, 573–588. https://doi.org/10.1016/j.rser.2013.08.090

Ziętek. (2022). The 9 colors of hydrogen—Learn about their meaning, use, and exploitation potential. *Ses Hydrogen*. https://seshydrogen.com/en/the-9-colors-of-hydrogen-learn-about-their-meaning-use-and-exploitation-potential/

Žigman, D., Tvorić, S., & Lonić, M. (2024). Comparative PSO Optimisation of Microgrid Management Models in Island Operation to Minimise Cost. *Energies*, *17*(16), 3901. https://doi.org/10.3390/en17163901

Zumdahl, S. S., & Zumdahl, S. A. (2000). *Chemistry* (5th ed., instructor's annotated ed.). Houghton Mifflin.

# Appendices

## Appendix 1. Load Profiles for Ammonia Production Plant (APP)

**Ammonia Production Plant (APP)**

| | | |
|---|---|---|
| **Ammonia needed** | **Mton** | **0.3** |
| Ammonia energy | GWh | 1446.7 |
| *Ammonia / hydrogen mass balance* | *-* | *5.52* |
| *Ammonia / nitrogen mass balance* | *-* | *1.19* |
| *Required electricity for ammonia production* | *MWh/ton* | *0.71* |
| Required electricity for ammonia production | GWh | 198.5 |
| **Hydrogen needed** | **Mton** | **0.05** |
| Hydrogen energy | GWh | 1690.8 |
| *Hydrogen / water mass balance* | *-* | *0.11* |
| *Hydrogen / oxygen mass balance* | *-* | *0.13* |
| *Electrolyser efficiency* | *%* | *65.0%* |
| Required electricity for hydrogen production | GWh | 2601.3 |
| Total electricity consumption | GWh | 2799.8 |
| Capacity factor | % | 40.0% |
| *Annual running hours* | *h* | *3504* |
| *Net electrical efficiency* | *%* | *100.0%* |
| **Required power capacity** | **GW** | **0.80** |
| | | |
| *Annual running hours for electrolyser* | *h* | *3504* |
| *Minimum electrolyser size* | *MW H2* | *483* |
| *Minimum electrolyser size* | *MW el* | *742* |

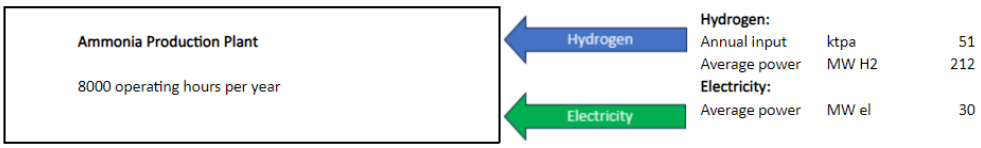

| **Additional, Non-Electrolysis Power Consumption** | | |
|---|---|---|
| Additional power consumption, of H2 production | % | 9% |
| Ammonia plant operating hours | h | 8000 |
| | | |
| Additional power consumption | GWh | 234.1 |
| Average power requirement | MW el | 29.3 |
| | | |
| Hydrogen | MJ/kg | 120 |
| Hydrogen | MWh/ton | 33.33333333 |
| Ammonia | MJ/kg | 18.6 |
| Ammonia | MWh/ton | 5.166666667 |

## Appendix 2. CAPEX and FOM for Components

| Component | CAPEX | FOM |
|---|---|---|
| Generic 1 MWh Lithium-Ion Battery | 225 $/kWh & 284 $/kW | 27.775 $/kWh |
| Hydrogen Tank | 600 $/kg | 24 $/kW |
| Generic Electrolyzer | 900 $/kW | 10 $/kW |
| System Converter | 50 $/kW | 0.5 $/kW |
| Generic 1.5 MW Wind Turbine | 1093,383 $/kW | 26.075 $/kW |
| Generic Solar Panel | 829,208 $/kW | 15.518 $/kW |

The CAPEX and FOM prices for the components used in Kalliovalkama's 2024 thesis are based on data from NREL.com (see sources above). These prices have been recalculated using referenced NREL data, assuming moderate scenarios for the year 2035 and a 30-year cost recovery period. For detailed information on specific components, please refer to the NREL website.

## Appendix 3. Case Study 1 Parameters for LCOE & LCOH

| Parameter | Unit | Value |
|---|---|---|
| Wind Capacity 24 | MW | 751.5 |
| Wind Annual Generation 24 | MWh | 3,284,987 |
| Solar Capacity 24 | MW | 632.438 |
| Solar Annual Generation 24 | MWh | 1113572 |
| BESS Capacity 24 | MWh | 463 |
| BESS Annual Generation 24 | MWh | 13,640.43 |
| Converter Capacity 24 | MW | 52.7 |
| Converter Annual Generation 24 | MWh | 15603.8376 |
| Annual Power Generation | MWh | 4,398,558 |
| Electrolyzer Capacity 24 | MW | 666.039 |
| Electrolyzer Annual Generation 24 | MWh | 2082041.91 |
| Annual Hydrogen Generation | MWh | 2,082,042 |
| | | |
| Capex WIND | $/kW | 1093.383 |
| FOM WIND | $/kW | 26.075 |
| Economic Life WIND | Years | 25 |
| Capacity Factor WIND | % | 49.90% |
| Capex SOLAR | $/kW | 829.208 |
| FOM SOLAR | $/kW | 15.518 |
| Economic Life SOLAR | Years | 25 |
| Capacity Factor SOLAR | % | 20.10% |
| Capex BESS | $/kWh | 225 |
| FOM BESS | $/kWh | 27.775 |
| Economic Life BESS | Years | 15 |
| Capex CONVERTER | $/kW | 50 |
| FOM CONVERTER | $/kW | 0.5 |
| Economic Life CONVERTER | Years | 20 |
| Capacity Factor CONVERTER 24 | % | 3.38% |
| Capex Electrolyzer | $/kW | 900 |
| FOM Electrolyzer | $/kW | 10 |
| Economic Life Electrolyzer | Years | 20 |
| Capacity Factor Electrolyzer 24 | % | 54.90% |
| Electrolyzer Efficiency | % | 65% |
| WACC | % | 8% |
| H2, LHV | MJ/kg | 120 |
| H2, LHV | MWh/kg | 33.3 |

## Appendix 4. Tasmania Renewable Resource Output Profiles

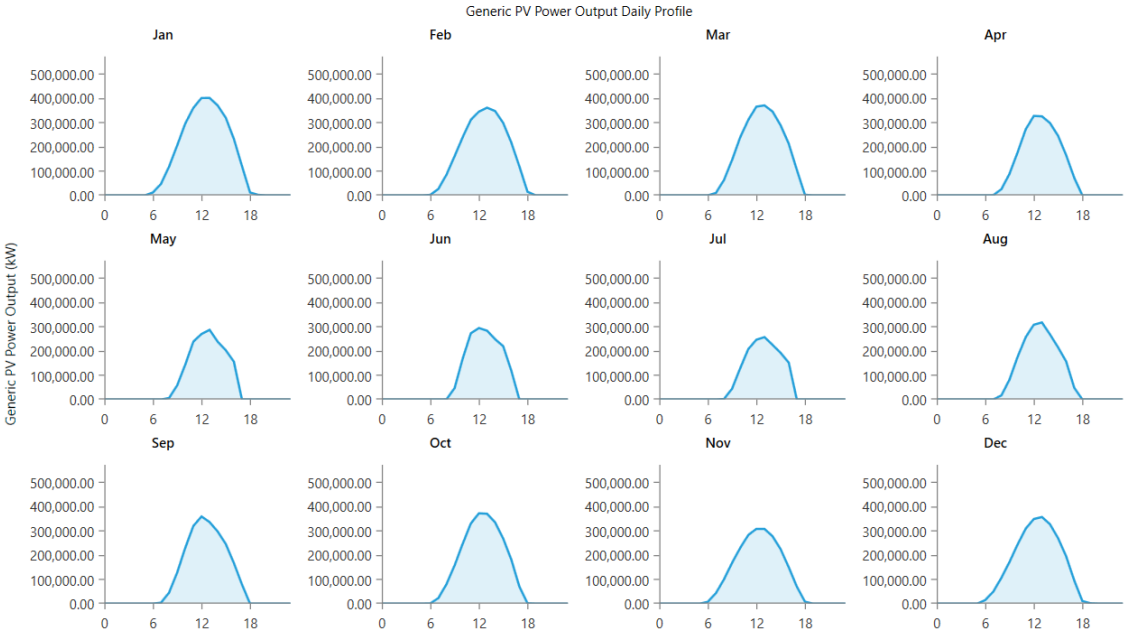


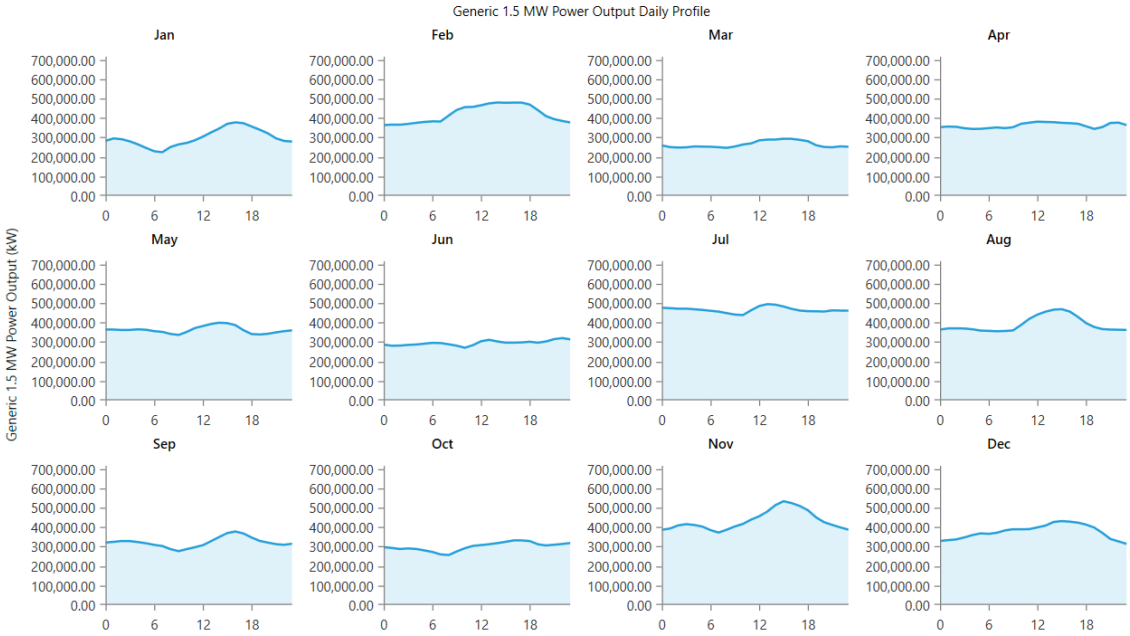


The figures above are screenshots, taken from HOMER Pro, of the results from Case Study 1, illustrating the output profiles of renewable resources in Tasmania. The solar resource is depicted in the upper figure, while the wind resource is shown in the lower figure.

## Appendix 5. Bolivia Renewable Resource Profiles

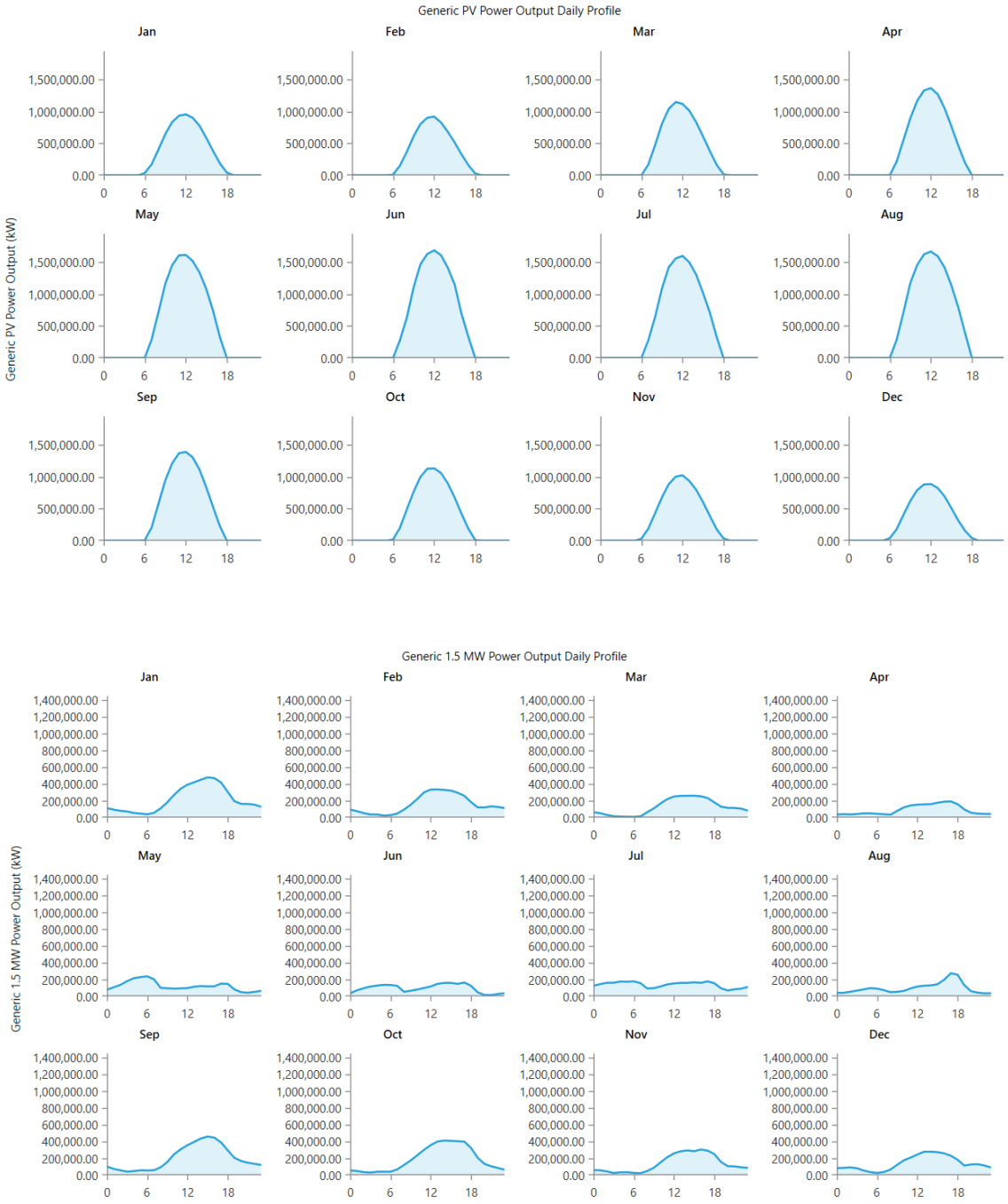


The figures above are screenshots, taken from HOMER Pro, of the results from Case Study 4, illustrating the output profiles of renewable resources in Bolivia. The solar resource is depicted in the upper figure, while the wind resource is shown in the lower figure.

## Appendix 6. Norway Renewable Resource Profiles


The figures above are screenshots, taken from HOMER Pro, of the results from Case Study 7, illustrating the output profiles of renewable resources in Norway. These profiles are identical across all three case studies conducted at this location. The solar resource is depicted in the upper figure, while the wind resource is shown in the lower figure.